Transplantation of Exosomes Derived From Human Wharton's Jelly Mesenchymal Stromal Cells Enhances Functional Improvement in Stroke Rats

Yu-Sung Chiu[1] [iD], **Kuo-Jen Wu[2], Seong-Jin Yu[3], Kun-Lieh Wu[1,4],
Chang-Yi Hsieh[1], Yu-Sheng Chou[1], Kuan-Yu Chen[1],
Yu-Syuan Wang[3], Eun-Kyung Bae[3], Tsai-Wei Hung[3],
Shih-Hsun Lin[5], Chih-Hsueh Lin[5], Shu-Ching Hsu[6,7,8,9,10],
Yun Wang[3], and Yun-Hsiang Chen[3,5]** [iD]

Abstract
Cerebral ischemic stroke is a major cerebrovascular disease and the leading cause of adult disability. We and others previously demonstrated that transplantation of human Wharton's jelly mesenchymal stromal cells (WJ-MSCs) attenuated neuronal damage and promoted functional improvement in stroke animals. This study aimed to investigate the protective effects of human WJ-MSC exosome (Exo) transplant in cellular and rat models of cerebral stroke. Administration of Exo significantly antagonized glutamate-mediated neuronal loss and terminal deoxynucleotidyl transferase (TdT)-mediated dUTP-X nick end labeling (TUNEL) in rat primary cortical neuronal cultures. Adult male rats underwent a 60-min middle cerebral artery occlusion (MCAo); Exo or vehicle was injected through the tail vein 5–10 min after the MCAo. Two days later, the rats underwent a series of behavioral tests. Stroke rats receiving Exo developed a significant improvement in locomotor function and forelimb strength while reductions in body asymmetry and Bederson's neurological score. After the behavioral test, brain tissues were harvested for histological and quantitative real-time reverse transcription polymerase chain reaction (qRT-PCR) analyses. Animals receiving Exo had less infarction volume, measured by 2,3,5-triphenyl tetrazolium chloride (TTC) staining. Transplantation of Exo increased the expression of protective neurotrophic factors (BMP7, GDNF) and anti-apoptotic factors (Bcl2, Bcl-xL) in the ischemic brain. These findings suggest that early post-treatment with WJ-MSC Exo, given non-invasively through the vein, improved functional recovery and reduced brain damage in the stroke brain.

Keywords
apoptosis, exosome, neurotrophic factor, mesenchymal stromal cell, stroke

Graphical Abstract
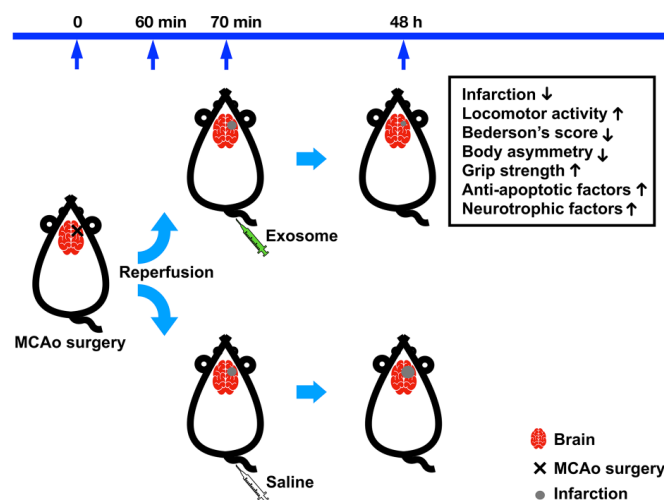
Introduction

Cerebral stroke is the second most fatal disease worldwide, with approximately 75% of its survivors experiencing permanent disabilities. It imposes heavy economic burdens on patients and society[1,2]. Cerebral ischemic stroke, usually caused by a blood clot that blocks blood circulation in the brain, accounts for 87% of the stroke population[3]. Cerebral ischemia leads to pathological reactions such as mitochondrial dysfunction, glutamate excitotoxicity, inflammation, and apoptosis, eventually causing neuronal damage in the brain[4,5]. Currently, the treatment for cerebral ischemic stroke is limited to rapid recanalization by endovascular thrombectomy and intravenous thrombolysis by injection of tissue plasminogen activator[6]. Medications to ameliorate cerebral ischemia-mediated neuronal degeneration are still limited. Developing adjunctive therapies to facilitate neuronal restoration in post-cerebral ischemic stroke is crucial and necessary.

Increasing evidence supports that mesenchymal stromal cell (MSC) transplant promotes neurogenesis, angiogenesis, and functional recovery in experimental stroke models[7,8]. We previously reported that intracerebral transplantation of human placenta–derived MSCs reduced activation of microglia and brain infarction in the stroke brain[9]. These transplants released trophic factors or cytokines, leading to protection, anti-inflammation, and repair[10–14]. MSCs can self-renew and have the potential to differentiate into various cell lineages of three germ layers: endoderm (endothelial cells and hepatocytes), mesoderm (adipocytes, chondrocytes, and osteoblasts), and ectoderm (neurons and glia cells)[15,16]. MSCs can be obtained from various tissues such as adipose tissue, bone marrow, cord blood, placenta, or tooth buds.

The human umbilical cord (hUC) has been increasingly considered a source of MSCs due to its abundant supply from discarded tissues and less ethical concerns[17,18]. We previously demonstrated that transplantation of MSCs from the human Wharton's jelly of the umbilical cord [Wharton's jelly mesenchymal stromal cell (WJ-MSCs)] attenuated neuronal damage and promoted functional improvement in stroke animals[19]. We also reported that the protective effect of these cells was indirectly mediated through the production of protective factors from the transplants[19].

The protective effects of MSCs may also be attributed to the exosomes (Exos) in the graft cells. A growing body of studies has suggested that MSC-derived Exos hold promise as a treatment for cerebral ischemic stroke[20,21]. Exo treatment reduces neuroinflammation[22,23], oxidative stress[24], and apoptosis[25] while promoting angiogenesis[26] and neuroregeneration[27] in the damaged brain. Further research is essential for a complete understanding of the underlying mechanism and to translate these findings into effective treatments for ischemic stroke patients.

Exos are lipid bilayer vesicles, typically 50–150 nm in diameter, produced by almost all types of cells, including MSCs, immune cells, and cancer cells[28]. Their surface is decorated with transmembrane proteins such as CD9, CD63, and CD81. The interior of Exos contains a diverse array of proteins, DNA, RNA, metabolites, and other bioactive substances, which can vary depending on the type of parental cells[29]. Exos are formed as intraluminal vesicles (ILVs) in multivesicular bodies (MVBs) through the inward budding of endosomal membranes[30]. When MVBs fuse with the cell membrane, Exos are released to the extracellular space as vesicles, through which they can transfer their cargo to other cells by membrane fusion or vesicle internalization[30]. In addition, Exos can cross the blood–brain barrier (BBB), as demonstrated in the rodent models that received intranasal or intravenous delivery of Exos loaded with catalase, recombinase, siRNA, or curcumin[31–34]. Due to their stability, biocompatibility, low immunogenicity, functional contents, and ability to cross BBB, Exos have the potential to be used as cell-free therapeutic agents for cerebral ischemic stroke.

This study aimed to investigate the protective effects of Exos derived from human WJ-MSCs in a rat model of cerebral ischemic stroke. We found that intravenous administration of WJ-MSC Exos after transient middle cerebral artery occlusion (MCAo) improved neurological function recovery and reduced brain damage in stroke rats. Our findings support that human WJ-MSC-derived Exo is potentially useful for the early post-treatment of ischemic stroke.

[1] YJ Biotechnology Co., Ltd., New Taipei City, Taiwan

[2] School of Pharmacy, College of Pharmacy, China Medical University, Taichung, Taiwan

[3] Center for Neuropsychiatric Research, National Health Research Institutes, Zhunan, Taiwan

[4] Department of Electrical Engineering, I-Shou University, Kaohsiung, Taiwan

[5] Department of Life Science, Fu-Jen Catholic University, New Taipei City, Taiwan

[6] Institute of Infectious Diseases and Vaccinology, National Health Research Institutes, Zhunan, Taiwan

[7] Graduate Institute of Medicine, College of Medicine, Kaohsiung Medical University, Kaohsiung, Taiwan

[8] PhD Program in Tissue Engineering and Regenerative Medicine, National Chung Hsing University, Taichung, Taiwan

[9] Immunology Research and Development Center, China Medical University, Taichung City, Taiwan

[10] Department of Life Sciences, Tzu Chi University, Hualien, Taiwan

Corresponding Author:
Yun-Hsiang Chen, Department of Life Science, Fu-Jen Catholic University, No. 510, Zhongzheng Road, Xinzhuang District, New Taipei City 24205, Taiwan.
Email: 125648@mail.fju.edu.tw

Materials and Methods

Human WJ-MSCs

Newborn umbilical cord tissues were collected from term deliveries of healthy donors who had signed the written informed consent. This study was approved by the Institutional Review Board (IRB) of Fu Jen Catholic University (approval no. C111157) and conducted in accordance with the Declaration of Helsinki. Donors' peripheral blood samples were tested negative for hepatitis B virus (HBV) antigens and antibodies against HIV1, HIV2, hepatitis C virus (HCV), and syphilis. The isolation and expansion of WJ-MSCs was undertaken within a Good Manufacturing Practice (GMP)-grade cell processing unit (#EZCPi ONE, YJ Biotechnology, New Taipei City, Taiwan) approved by the Taiwan Food and Drug Administration (TFDA) under the regulations of Good Tissue Practice (GTP). The umbilical cord specimen was collected in a sterile bottle filled with Hank's balanced salt solution (HBSS) supplemented with antibiotics (streptomycin 100 μg/ml, penicillin 100 IU/ml) and processed for culturing WJ-MSCs within 24 h. After removing the umbilical arteries, veins, and adventitia, we sliced Wharton's jelly tissues into pieces smaller than 1 mm^3. The slices were treated with collagenase type II at 37°C in a humidified incubator with 5% CO_2 for 18 h. Cells were harvested by centrifugation and grown in Iscove's Modified Dulbecco's Medium (IMDM) supplemented with 5% human platelet lysate (hPL) at 37°C in a humidified incubator with 5% CO_2. Flow cytometry analysis confirmed the expanded cells expressing high levels of MSC surface markers (CD73, CD90, and CD105) but no hematopoietic stem cell marker (CD34).

Exosome Purification

The conditioned media of human WJ-MSCs cultures was harvested and centrifuged at 4,000 × *g* for 10 min, followed by filtration through a 0.22-μm filter to remove cell debris and larger particles. The clarified conditioned media was circulated through a tangential flow filtration (TFF) device (0.05 μm pore size) by a peristaltic pump to reduce the volume by 10 folds. The ultrafiltrated media was subjected to exosome (Exo) purification using the exoEasy Maxi kit (#76064; Qiagen; Hilden, Germany) per the manufacturer's written instructions. Briefly, the ultrafiltrated media was mixed with an equal volume of binding buffer and applied into a membrane-based spin column. After centrifugation at 4,000 × *g* for 1 min, the column was washed once with 10 ml of washing buffer, followed by centrifugation at 4,000 × *g* for 5 min. The bound Exos were eluted from the column with 2 ml of elution buffer by centrifugation at 4,000 × *g* for 5 min. The eluates were concentrated in saline to 0.5 ml using an ultrafiltration spin column (100 kDa MWCO; Cytiva; Uppsala, Sweden). The purified Exos were aliquoted and stored at −80°C until use.

Western Blot Analysis

Lysates of human WJ-MSCs and Exos were prepared for Western blot analysis as previously described[35,36]. Briefly, WJ-MSCs ($8 × 10^5$ cells) or Exos ($2 × 10^{10}$ ptc) were resuspended in 100 μl of phosphate-buffered saline (PBS) and mixed with 100 μl of 2× Laemmli buffer (125 mM Tris-HCl pH 6.8, 20% glycerol, 10% β-mercaptoethanol, 4% sodium dodecyl sulfate (SDS), and 0.004% bromophenol blue in distilled water), followed by passing through a 25-gauge needle 20 times to reduce viscosity. After being heated at 90°C for 10 min, the Laemmli buffer–treated samples were subjected to electrophoresis separation on 12% SDS-polyacrylamide gels. The separated proteins were transferred from the gel to a polyvinylidene fluoride (PVDF) membrane (#RPN303F; GE HealthCare; Buckinghamshire, UK) by electrophoresis. The membrane was then incubated with 10-ml blocking buffer (5% skim milk and 0.1% Tween-20 in PBS) for 1 h and then incubated with appropriate primary antibodies in 3-ml blocking buffer (in a 50-ml centrifuge tube) at 4°C overnight with gentle rotation. Six rabbit monoclonal antibodies against five exosome markers CD9 (1:2,000, #ab263091; Abcam), CD63 (1:2,000, #ab134045; Abcam), CD81 (1:2,000, #ab109201; Abcam), Hsp70 (1:2,000, #ab181606; Abcam), and TSG101 (1:2,000, #ab125011; Abcam) and one endoplasmic reticulum marker Calnexin (1:2,000, #ab133615; Abcam), and one mouse monoclonal antibody against a cellular housekeeping protein β-actin (1:3,000, #GTX629630; GeneTex) were used as primary antibodies. After washing with 0.1% Tween-20 (in PBS) three times for 10 min each, the membrane was incubated with horseradish peroxidase (HRP)-conjugated goat polyclonal antibodies against mouse IgG (1:2,500; #GTX213111-01; GeneTex) or rabbit IgG (1:2,500; #GTX213110-01; GeneTex) in 3-ml blocking buffer for 1 h, followed by the washing procedure described above. The target proteins on the membrane were detected using an enhanced chemiluminescence reagent (##GTX14698; GeneTex), and the light emission signals were captured by the CCD camera-based image system MultiGel-21 (TOPBIO, New Taipei City, Taiwan). The intensity of the detected images was quantified by ImageJ software (http://imagej.net).

Exosome Particle Analysis

The purified Exos were analyzed by nano-flow cytometry (nFCM) to determine particle size, concentration, and surface markers. Samples were diluted in PBS to the concentration, achieving a flow rate within an optimal range of 2,000–12,000 counts per minute. Based on the calibration curve, the particle size and concentration were determined by converting the flow rate and side scattering intensity using NanoFCM software (NanoFCM, Profession V2.315). For the detection of Exo surface markers, samples were stained with fluorescent dye–conjugated monoclonal antibodies against CD9, CD63, or CD81 at

37°C for 1 h. After centrifugation at $100,000 \times g$ at 4°C, Exo pellets were washed once with PBS and resuspended in PBS for phenotype analysis by nFCM. In addition, the particle size, concentration, and surface markers of exosomes from 5% hPL-supplemented fresh medium and WJ-MSC conditioned medium were examined using the ZetaView MONO system (Particle Metrix; Ammersee, Germany).

Transmission Electron Microscopy

The Exo resuspension (10 μl, in PBS) was added to a carbon-coated grid for 60 s. The grid was blotted with filter papers to remove the excessive solution, followed by conventional negative staining with 1% uranyl acetate (10 μl) for 90 s. After blotting with filter papers, the grid was washed once with distilled water (20 μl) and left to air-dry for 20 min. Exo images were recorded using a transmission electron microscope (JEM-1400, JEOL) operated at an acceleration voltage of 120 kV.

Animals

Adult male Sprague-Dawley rats were purchased from BioLASCO Co., Ltd. (Taipei, Taiwan) and housed in an environment with controlled conditions: light on at 7:00 and off at 19:00, constant room temperature at $24 \pm 2°C$, and relative humidity at $50 \pm 10\%$. All animals habituated for 2 weeks after their arrival and had free access to drinking water and autoclaved food. Animal experiments were conducted under the protocol approved by the Animal Research Ethics Board at the National Health Research Institutes in Taiwan (approval no. NHRI-IACUC-112034-A). We have carefully read and adhered to the ARRIVE guidelines.

In this exploratory study, we aimed to investigate whether human WJ-MSC Exos can attenuate neuronal damage caused by cerebral ischemic stroke. The sample size of each group in a two-sided *t*-test comparison was chosen based on assuming an alpha level of 0.05, a power of 90% chance of detecting the effect, and an effect size of 1.6 standard deviation units[37]. Given the attrition and unexpected loss of animals or data during the experiment, we increased the sample size by 20%. Therefore, a total of 12 rats per group was considered necessary. The random numbers were generated using the RAND function of Mac's *Numbers* application to allocate rats to experimental groups. A total of 29 rats (male, 3 months old) were randomly separated into three groups: naive ($n = 5$), stroke surgery followed by the treatment with saline ($n = 12$), or Exos ($n = 12$). One animal of the saline-treated group died during the stroke surgery. The researchers who conducted the animal experiments were aware of the group allocation, but the animal care staff and the researchers who analyzed the data were unaware of it.

Primary Cortical Neuronal Cultures

The brain cortex tissues were aseptically collected from fetuses (at embryonic days 14–15) of timed-pregnant rats (Sprague-Dawley). After removing the meninges and blood vessels, the dissected cortices were pooled and treated with 0.05% trypsin at room temperature for 20 min. Cells were harvested by low-speed centrifugation and rinsed with pre-warmed Dulbecco's modified Eagle's medium (DMEM) to remove trypsin. Cell pellets were dissociated in the neuron culture medium by repeatedly pipetting and then grown in a 96-well plate, which was precoated with poly-D-lysine (Sigma; St Louis MO, USA), at a density of 5×10^4 cells/100 μl/well at 37°C in a humidified incubator with 5% CO_2. The neuron culture medium comprises the Neurobasal medium (Invitrogen) supplemented with 2% B27, 0.5 mM L-glutamine, 0.025 mM L-glutamate, and 2% heat-inactivated fetal bovine serum (FBS). Half volume of the culture medium was replaced with the Feed medium (Neurobasal medium supplemented with 2% B27 and 0.5 mM L-glutamine) plus antioxidants on days *in vitro* (DIV) 3 and 5. On DIV7, half the volume of the culture medium was replaced with the Neurobasal medium supplemented with 2% B27. On DIV10, 50 μl of culture medium was replaced with 50 μl of saline (as control) or saline supplemented with 200 μM glutamate, 200 μM glutamate + 5×10^8 ptc of Exos, or 200 μM glutamate + 5×10^9 ptc of Exos. On DIV12, cells were fixed with 4% paraformaldehyde (PFA) for immunocytochemistry and terminal deoxynucleotidyl transferase (TdT)-mediated dUTP-X nick end labeling (TUNEL) analyses.

Immunocytochemistry

PBS was used in the washing step, and antibodies were diluted in PBS. The primary cortical neuron (PCN) cells grown in a 96-well plate were fixed with 4% PFA. After washing once, cells were permeabilized by incubating with 100 μl of blocking solution (composed of 5% bovine serum albumin, 0.1% Triton X-100, and 1× PBS) for 1 h. After washing once, cells were incubated with a mouse monoclonal antibody against MAP2 (1:500; #MAB3418; Millipore; Darmstadt, Germany) at 4°C overnight. After washing three times, cells were incubated with an Alexa Fluor 488-conjugated goat antibody against mouse IgG (1:1,000; Invitrogen) for 2 h. After washing three times, cells were examined by an inverted fluorescence microscope Nikon Eclipse Ti1 (Nikon) using an excitation wavelength of 450–500 nm and a detection wavelength of 515–565 nm (green). Images (10× magnification) were acquired from four fields per well by a camera DS-Qi2 (Nikon) and analyzed using NIS Elements AR 5.11 Software (Nikon).

Terminal Deoxynucleotidyl Transferase (TdT)-Mediated dUTP-X Nick End Labeling

The PCN cells grown in a 96-well plate were analyzed for DNA fragmentation using the In Situ Cell Death Detection Kit (#11684795910; Roche; Indianapolis IN, USA) per the

manufacturer's instructions. Briefly, cells were fixed with 4% PFA and, after washing once, incubated with 0.1% Triton-X 100 (in 0.1% sodium citrate) on ice for 2 min to permeabilize the cell membrane. After washing twice, cells were incubated with 50 µl of TUNEL reaction mixture for 60 min at 37°C in a humidified chamber. After washing three times, cells were examined by an inverted fluorescence microscope Nikon Eclipse Ti1 (Nikon) using an excitation wavelength of 450–500 nm and a detection wavelength of 515–565 nm (green). Images (20× magnification) were acquired from four fields per well by a camera DS-Qi2 (Nikon), and TUNEL$^+$ cells were manually counted.

Transient MCAo

Rats (male, 3 months old; $n = 24$) were anesthetized by intraperitoneal (i.p.) injection with sodium pentobarbital (35 mg/kg). A burr hole of about 2–4 mm in diameter was made using a dental drill in the right squamosal bone. Afterward, common carotids were clamped bilaterally by arterial clips, and the right distal middle cerebral artery (MCA) was ligated with a 10-0 nylon suture. After 60-min ischemia, the suture and arterial clips were removed to restore blood supply and generate cerebral ischemia-reperfusion injuries. One animal died on the table during the surgery. Rats were administered with 0.5 ml of saline ($n = 11$) or human WJ-MSC Exos (10^{11} ptc/ml; $n = 12$) via the tail-vein injection 5–10 min after reperfusion. Rats were kept in an incubator at 37°C until recovering from anesthesia.

Locomotor Activity Test

Rats (naive, $n = 5$; MCAo/saline, $n = 11$, MCAo/Exo, $n = 12$) were individually placed in transparent acrylic chambers (42 cm × 42 cm × 30 cm; length × width × height), equipped with infrared sensors aligned in the horizontal and vertical directions (AccuScan Instruments, Inc.). After rats habituated for 30 min, the locomotor activity data were collected by recording the events of beam interruption for 2 h during the light cycle (2 p.m.–4 p.m.). Six parameters were measured, including horizontal activity (HACTV; the number of beam interruptions detected by the horizontal sensors), total distance traveled (TOTDIST; distance traveled by the animals), movement numbers (MOVNO; the counts of horizontal movements followed by a break lasting over one second), movement time (MOVTIME; the total time when the animal was detected moving), vertical activity (VACTV; the number of beam interruptions detected by the vertical sensors), vertical movement number (VMOVNO; the number of vertical movements followed by a period during which the animal must go below the level of the vertical sensor for at least one second), and vertical movement time (VTIME; the total time when the animal was detected moving vertically).

Body Asymmetry Test

Rats (naive, $n = 5$; MCAo/saline, $n = 11$, MCAo/Exo, $n = 12$) were examined for lateral movement using the elevated body swing test[38,39] when suspended 20–30 cm above the table by lifting their tails. The frequency of the turning of the head or upper body opposite to the lesion brain side was counted in 20 consecutive trials. The stroke rats presented asymmetric lateral movement with almost 20 turns per 20 trials, while the naive rats showed almost equal frequency in each direction.

Modified Bederson's Neurological Test

Rats (naive, $n = 5$; MCAo/saline, $n = 11$, MCAo/Exo, $n = 12$) were assessed for the degree of neurological deficits, graded on a scale of 0–3 when suspended 20–30 cm above the table by lifting their tails[39,40]. If rats stretch both forelimbs toward the table, grade 0 (no observable deficit) is assigned. If rats draw one forelimb back to the breast and extend the other forelimb straight, grade 1 is assigned. In addition to the behavior in grade 1, if rats exhibit decreased resistance to lateral push and display no circling, grade 2 is assigned. In addition to the behavior in grade 2, if rats twist the upper half of their body, grade 3 is assigned.

Grip Strength Test

Forelimb strength was assessed by a grip strength meter (#BIO-GS3; Bioseb). Rats (naive, $n = 5$; MCAo/saline, $n = 7$, MCAo/Exo, $n = 6$) were positioned horizontally over the grid of the grip strength meter to allow their right or left forepaws to attach to the top portion of the grid stably. When the rat grasped the grid, it was pulled by the root of the tail away from the grid. The maximal grip strength value displayed in grams was recorded by the grip strength meter. After three consecutive trials, the mean value of each forelimb of each rat was calculated.

2,3,5-Triphenyl Tetrazolium Chloride Staining

Two days after MCAo, rats were decapitated. The collected brains (MCAo/saline, $n = 7$, MCAo/Exo, $n = 6$) were sliced into 2-mm-thick sections, which were immersed in PBS supplemented with 2% 2,3,5-triphenyl tetrazolium chloride (TTC, #T8877; Sigma) at room temperature for 15 min and then fixed in 4% PFA for 20 min. The images of stained brain slides were taken with a digital scanner, and infarction areas were measured using the ImageJ software. The infarction

Table 1. Oligonucleotide Primers and Probes Used for qRT-PCR.

Gene	Forward (5′—3′)	Reverse (5′—3′)	[a]TaqMan probe
	Primers for SYBR green detection		
Bcl2	GATTGTGGCCTTCTTTGAG	CAAACTGAGCAGAGTCTTC	
Bcl-xL	CAGAGCTTTGAACAGGTAG	GCTCTCGGGTGCTGTATTG	
BDNF	CACTTTTGAGCACGTCATCG	TCCTTATGGTTTTCTTCGTTGG	
BMP7			Rn10528889_m1
GDNF	TAAGATGAAGTTATGGGATGTCG	CTTCGAGAAGCCTCTTACCG	
CD86	TAGGGATAACCAGGCTCTAC	CGTGGGTGTCTTTTGCTGTA	
CD206	AGTTGGGTTCTCCTGTAGCCCAA	ACTACTACCTGAGCCCACACCTGCT	
IL1β	CCAGGATGAGGACCCAAGCA	TCCCGACCATTGCTGTTTCC	
IL6	GACCAAGACCATCCAACT	TAGGTTTGCCGAGTAGAC	
IL10	AAAGCAAGGCAGTGGAGCAG	TCAAACTCATTCATGGCCTTGT	
TGFβ	GCTGAACCAAGGAGACGGAAT	CGGTTCATGTCATGGATGGTG	
TNFα	CCACACCGTCAGCCGATT	TCCTTAGGGCAAGGGCTCTT	
GAPDH			Rn01775763_g1

[a]The TaqMan probes targeting BMP7 and GAPDH were purchased from ThermoFisher Scientific, but the primer sequences were not revealed in the kit.

volume was obtained by multiplying the sum of infarction areas and the average thickness (2 mm) of brain slides.

RNA Extraction

Cortical tissues of the infarcted or non-infarcted brain hemisphere (MCAo/saline, $n = 11$, MCAo/Exo, $n = 12$) were subjected to RNA extraction by Trizol Reagent (#15596-018; Ambion) according to the manufacturer's instruction[41]. Briefly, each cortical tissue was lysed with 0.4 ml of Trizol reagent, and the lysate was homogenized by pipetting up and down several times. After incubation on ice for 5 min, the lysate was mixed with 80 μl of chloroform, followed by incubation on ice for 3 min. After centrifugation at $12,000 \times g$ at 4°C for 15 min, the upper aqueous phase containing the RNA was transferred to a 1.5-ml microcentrifuge tube and mixed with 0.2 ml of isopropanol. After incubation on ice for 10 min, the sample was centrifuged at $12,000 \times g$ at 4°C for 10 min. The precipitated RNA pellet was washed once with 0.4 ml of 75% ethanol, air-dried for 10 min, and resuspended in 30 μl of RNase-free water (#10977-015; Invitrogen). To degrade potentially contaminated DNA fragments, we treat the resuspended RNA with two units of DNase I (#M0303S, NEB) in 100 μl of 1× DNase I reaction buffer at 37°C for 10 min. RNA was then re-extracted by chloroform, re-precipitated by isopropanol, and washed by ethanol, as described above. Finally, the purified RNA was quantified by a NanoDrop spectrophotometer and stored at −80°C until use. One animal's cortical samples of the MCAo/Exo group were excluded due to the failure of RNA extraction.

qRT-PCR Analysis

The mRNA levels of selected genes, listed in Table 1, were determined by quantitative real-time reverse transcription polymerase chain reaction (qRT-PCR) performed on an ABI StepOnePlus system. First, the purified total RNA of each sample (MCAo/saline, $n = 11$, MCAo/Exo, $n = 11$) was transcribed into cDNA using the RevertAid First Stand cDNA Synthesis Kit (#K1622; ThermoFisher Scientific). Briefly, the RNA (1 μg) was mixed with 1 μl of random hexamer primers (100 μM) in distilled water to a volume of 12 μl and then incubated at 65°C for 5 min, followed by chilling on ice. Next, 4 μl of 5× reaction buffer, 2 μl of dNTP (10 mM), 1 μl of RNase inhibitor (20 U/μl), and 1 μl of M-MuLV reverse transcriptase (200 U/μl) were added to the chilled mixtures. The total mixture (20 μl) was incubated at 25°C for 5 min, followed by 42°C for 60 min. Finally, the reaction was terminated by heating at 70°C for 5 min. A 40-fold dilution of the resulting cDNA was made in distilled water. The mRNA levels of most of the selected genes were determined by SYBR Green-based qPCR. Briefly, 2 μl of diluted cDNA, 10 μl of 2× SYBR Green PCR master mix (#K0371; ThermoFisher Scientific), and 2 μl of each primer (5 μM) were mixed in distilled water to a final volume of 20 μl. The PCR cycling program was set as follows: 50°C for 2 min and 95°C for 10 min, followed by 40 cycles of denaturation at 95°C for 15 s and annealing/extension at 60°C for 1 min. The primer sequences used for the PCR were designed by the Primer-3 program and listed in Table 1. The specificity of PCR products was verified by performing a melting-curve analysis (95°C for 15 s, 60°C for 1 min, and 95°C for 15 s) at the end of the PCR. The mRNA levels of GAPDH and BMP7 genes were determined using commercially available primers and probes per the manufacturer's instructions. Briefly, a mixture containing TaqMan Fast Advanced Master Mix (5 μl), TaqMan probe (0.5 μl), distilled water (2.5 μl), and diluted cDNA (2 μl) was prepared. The PCR cycling program was set as follows: 95°C for 20 s, followed by 40 cycles of denaturation at 95°C for 1 s and annealing/extension at 60°C for 20 s. The mRNA levels of examined genes were normalized to that of the reference gene GAPDH and presented as fold changes using the $2^{-\Delta\Delta Ct}$ method[42].

MicroRNA Sequencing

Total RNA was isolated from WJ-MSC Exos using the miR-NAeasy kit (Qiagen), followed by the construction of microRNA (miRNA) libraries utilizing the QIAseq miRNA Library Kit (Qiagen). Next-generation sequencing was performed on the Illumina NovaSeq 6000 platform with a sequence depth of 20 million raw reads per sample to assess the quantity and sequence profiles of the miRNA molecules.

Protein Array

Total proteins were extracted from WJ-MSC Exos using radio-immunoprecipitation assay (RIPA) buffer, and the levels of 40 cytokines and 40 growth factors were quantified using multiplexed sandwich enzyme-linked immunosorbent assay (ELISA)-based arrays. Specifically, the Quantibody Human Inflammation Array 3 (#QAH-IFN-3; RayBiotech; Norcross GA, USA) and Quantibody Human Growth Factor Array 1 (#QAH-GF-1; RayBiotech; Norcross GA, USA) were employed. Protein signals labeled with Cy3 dye were scanned using an Innopsys InnoScan laser scanner. The concentrations of the target proteins were determined by comparing the signals from the samples against a standard curve.

Statistical Analysis

All data were presented as mean values $\pm$ standard error (SEM) and analyzed using GraphPad Prism 9.2.0 statistical software (GraphPad Software, Inc.). The infarction volume and locomotor activity between the Exo-treated and vehicle-treated groups were compared using the unpaired, two-tailed Student's *t*-test. In the qRT-PCR analysis, the difference in examined genes among groups was determined by ordinary one-way analysis of variance (ANOVA), followed by Tukey's multiple comparison test. The percentages of MAP2$^+$ counts and TUNEL$^+$ counts among groups treated with different doses of Exos and glutamate were compared using one-way ANOVA, followed by post hoc Dunnett's multiple comparison test. The assessments of neurological deficits, including Bederson's score, body asymmetry, and forelimb grip strength, were compared among groups using one-way ANOVA, followed by post hoc Dunnett's test. Statistical significance is considered when the *P* value is less than 0.05.

Results

Characterization of Human WJ-MSC Exos

Cells isolated from Wharton's jelly of hUCs were grown as monolayer cells attaching to the surface of culture vessels. They exhibited a liner and stretch morphology similar to that seen in fibroblasts (Fig. 1A). After trypsinization, cells were examined by flow cytometry and confirmed to express MSC surface markers (CD73, CD90, CD105) at high percentages

(>95%) (Fig. 1B–D) but almost no hematopoietic stem cell marker (CD34; <2%) (Fig. 1E). This finding is consistent with previous studies on the characterization of human WJ-MSCs[43–45]. Vesicles were purified from the conditioned medium of human WJ-MSC cultures by combining ultrafiltration and affinity adsorption methods, as previously described[46,47]. Transmission electron microscopy showed that the purified vesicles have a typical spherical shape (Fig. 2A). By nFCM, vesicle size was detected in the range of 45–180 nm with an average diameter of 73.0 $\pm$ 24.5 nm (Fig. 2B), and typical Exo surface markers (CD9, CD63, CD81) were found on the vesicle surface (Fig. 2C–F). Western blot analysis revealed that these vesicles contained Exo markers (CD9, CD63, CD81, HSP70, TSG101) but no endoplasmic reticulum marker (Calnexin) (Fig. 2G). These results indicated that human WJ-MSCs were successfully isolated from hUCs, and WJ-MSC-derived Exos were purified without contamination of endoplasmic reticulum components.

We recognize the concern about potential contamination from exosomes present in the 5% hPL-supplemented medium. To address this issue, we carefully monitored the exosome yield and characteristics to differentiate between exosomes from WJ-MSCs and those originating from hPL. After 6 days of WJ-MSC culture, the exosome concentration in the conditioned medium increased from 2.2×10^{10} ptc/ml (present in the fresh medium) to 4.1×10^{10} ptc/ml ($P = 0.0055$; Fig. 2H), with a reduction in mean particle size from 110 ± 0.4 nm to 91 ± 0.9 nm ($P = 0.003$) (determined by ZetaView, Fig. 2I). Over time, WJ-MSCs likely absorb or degrade exosomes from their culture medium, resulting in a higher portion of MSC-derived exosomes in the conditioned medium. In addition, we observed a significant increase in the percentage of exosomes expressing the surface marker CD9, from $27 \pm 3\%$ in the fresh medium to $46.5 \pm 1.5\%$ in the conditioned medium ($P = 0.0283$) (determined by ZetaView, Fig. 2J). Moreover, the miRNA profiles of exosomes purified from the conditioned medium (Fig. 7A) were markedly different from those of hPL-derived exosomes. Specifically, the seven most abundant miRNAs in the WJ-MSC-derived exosomes are distinct from those typically found in hPL exosomes[48,49]. These findings suggest that exosomes in the conditioned medium are primarily derived from WJ-MSCs rather than hPL.

WJ-MSC-Derived Exos Attenuated Glutamate-Induced Neurodegeneration and Apoptosis in PNC Culture

Cerebral ischemia leads to neuronal death in the brain, which is partly attributed to the release of excitatory amino acids[50–52]. The protective effects of human WJ-MSC-derived Exos against glutamate-mediated neurotoxicity were examined in the PNCs (Fig. 3). Cells were treated with saline (as control),
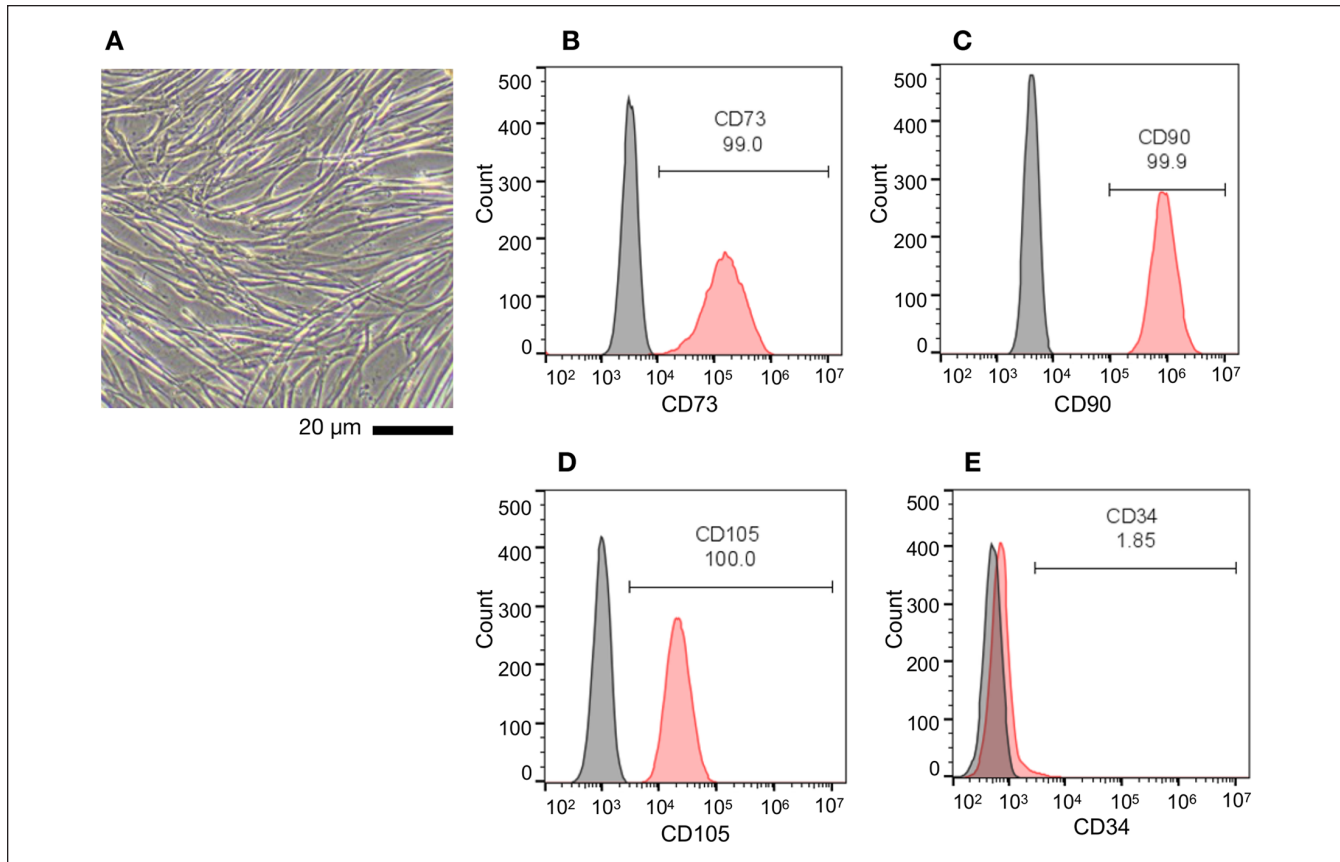
Figure 1. Characterization of human WJ-MSCs. (A) Phase-contrast image depicting the morphology of WJ-MSCs. Cells are observed as an adherent monolayer on the surface of a culture dish and display fibroblast-like morphology. Scale bar: 20 μm. (B—E) Cells were analyzed for specific surface markers by flow cytometry using fluorescein-conjugated antibodies targeting MSC surface markers (CD73, CD90, CD105) and a hematopoietic stem cell marker (CD34).

glutamate (Glu), or Glu + WJ-MSC Exos (Exo) at different concentrations for 48 h. Similar to previous reports[53,54], Glu (100 μM) significantly reduced Microtubule-Associated Protein 2 (MAP2) immunoreactivity (100 ± 5.4% vs 53.3 ± 2.9%, $P < 0.0001$) and increased TUNEL-positive cell counts (100 ± 8.8% vs 307.5 ± 6.0%, $P < 0.0001$), compared with the control. Administration of Exos significantly and dose-dependently increased MAP2 immunoreactivity (Fig. 3A, C; ×1 Exo: 74.6 ± 3.2%, $P = 0.0029$; ×10 Exo: 85 ± 3.7%, $P < 0.0001$) and antagonized Glu-mediated TUNEL (×1 Exo: 126.6 ± 6.0%, $P < 0.0001$; ×10 Exo: 124.1 ± 6.5%, $P < 0.0001$; Fig. 3B, D). These results suggest that WJ-MSC Exo protects PNCs from glutamate-mediated neurodegeneration and apoptosis.

WJ-MSC Exos Improved Motor Activity and Reduced Neurological Deficits in Stroke Rats

Stroke rats were transplanted with WJ-MSC Exos (Exo) or saline (Veh) via the tail vein 5–10 min after MCAo. Two days later, rats were individually placed in the activity chamber to record locomotor activity for 2 h (Fig. 4A, B).

The stroke rats receiving saline ($n = 11$) or Exos ($n = 12$; 5×10^{10} ptc of exosomes per animal) exhibited lower locomotor activity than naive rats ($n = 5$) (Fig. 4B). However, Exos significantly increased locomotor activity in stroke animals (Exo vs Veh; HACTV: 9,614 ± 689 vs 7,607 ± 589, $P = 0.0395$; TODIST: 3,655 ± 315 vs 2,811 ± 205, $P = 0.0391$; MOVNO: 354 ± 23 vs 288 ± 24, $P = 0.0635$; MOVTIME: 370 ± 23 vs 315 ± 24, $P = 0.1199$; VACTV: 1,127 ± 100 vs 812 ± 54, $P = 0.0133$; VMOVNO: 146 ± 10 vs 117 ± 8, $P = 0.0339$; VTIME: 397 ± 39 vs 262 ± 21, $P = 0.007$) (Fig. 4B). Two neurological tests were conducted. The stroke rats receiving saline ($n = 11$) or Exos ($n = 12$) had higher Bederson's neurological scores and body asymmetry than the naive rats ($n = 5$) (Fig. 4C, D). Exos significantly reduced Bederson's scores (Exo vs Veh; 1.75 ± 0.18 vs 2.46 ± 0.16, $P = 0.0073$) and body asymmetry (Exo vs Veh; 16.58 ± 0.61 vs 18.82 ± 0.44, $P = 0.0074$) in the stroke rats (Fig. 4C, D). Forearm strength was examined by the grip test. The stroke rats receiving saline ($n = 7$) or Exos ($n = 6$) had weaker grip strength than the naive rats ($n = 5$, Fig. 4E). Compared with saline, Exos improved the grip strength (411 ± 24 vs. 305 ± 21, $P = 0.005$, Fig.
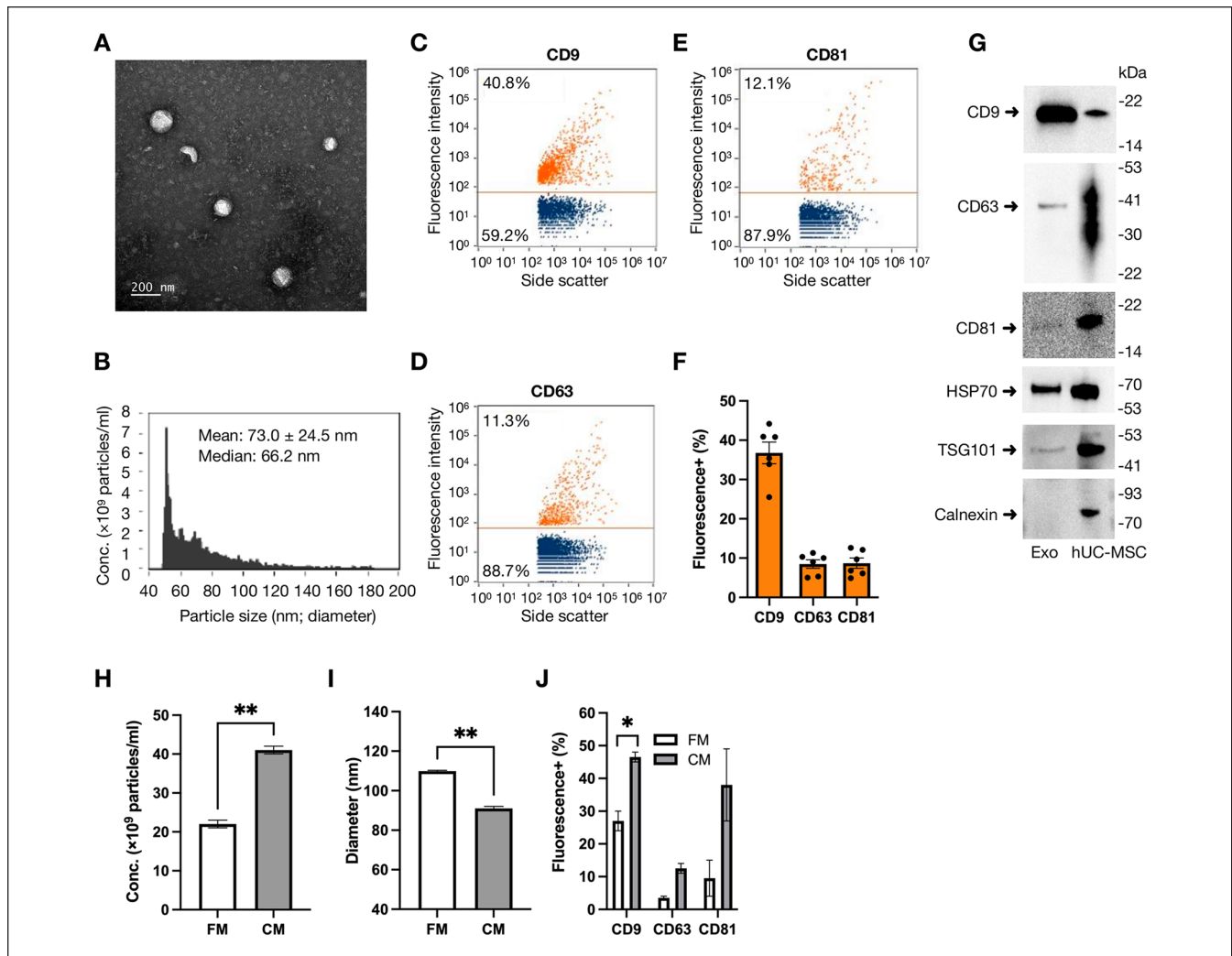
Figure 2. Characterization of Exos. Exos were purified from the culture medium of WJ-MSCs. (A) Exos were photographed under transmission electron microscopy. Scale bar: 200 nm. (B–F) Exos were further analyzed by nano-flow cytometry for particle concentration, size distribution (B), and surface markers. A set of representative dot plots revealed the percentage of Exos positive for the surface markers probed by fluorescein-labeled antibodies against CD9 (C), CD63 (D), and CD81 (E). (F) A statistical graph presented the percentage counts of indicated markers obtained from six batches of purified exosomes. Data were expressed as mean ± SEM. (G) Exo and WJ-MSC lysates were examined by Western blot analysis to detect protein markers of Exo (CD9, CD63, CD81, HSP70, TSG101) and endoplasmic reticulum membrane (Calnexin). The molecular weight (kDa) and migration location of protein markers were indicated. The hPL-supplemented fresh medium (FM) and conditioned medium (CM) collected from WJ-MSC cultures were examined by the ZetaView particle analyzer to determine the concentration (H), particle size (I), and surface markers (J) of exosomes in the medium. Duplicated results are presented as mean ± SEM, and significant differences between groups are indicated (*P < 0.05; **P < 0.01; Student's *t*-test).

4E). These results suggest that intravenous WJ-MSC Exos improved functional recovery in stroke animals.

Transplantation of WJ-MSC Exos Mitigated Brain Infarction

A total of 13 stroke rats were used in this study. Human WJ-MSC Exos (Exo; *n* = 6) or saline (Veh; *n* = 7) was given through the tail vein 5–10 min after MCAo. Brain tissues were collected for TTC staining 2 days after MCAo. As seen in Fig. 5, infarct volume was significantly reduced in animals

receiving Exos (64.1 ± 16.8 mm^3 vs 112.5 ± 12.5 mm^3, P = 0.0382; Fig. 5A, B), suggesting that intravenous administration of WJ-MSC Exos reduces brain infarction.

WJ-MSC Exo Transplants Increased the Expression of Anti-Apoptotic Factors (Bcl2, Bcl-xL) in the Ischemic Brain Cortices

Adult rats were subjected to the MCAo and administered either saline (Veh; *n* = 11) or WJ-MSC Exos (Exo; *n* = 11) via the tail vein. Two days after MCAo, the cortical tissues of
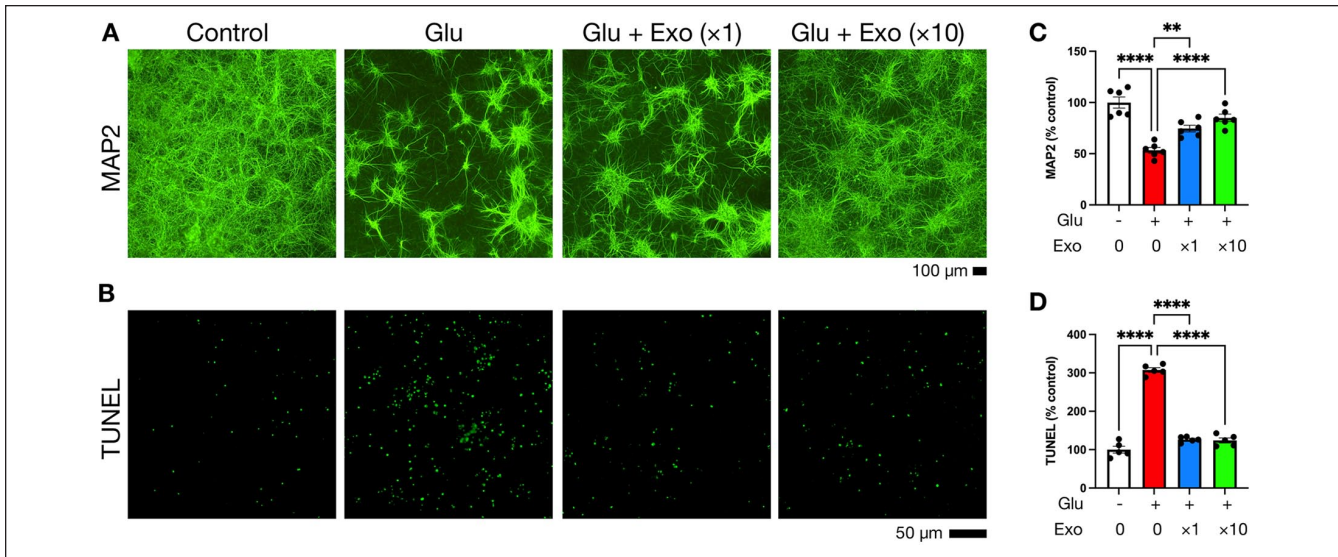
Figure 3. Exos protect cortical neurons from excitotoxicity. Rat primary cortical neurons were grown in a 96-well plate for 10 days and then treated with saline (as control), glutamate (Glu; 100 μM), or Glu + WJ-MSC Exos at different concentrations (×1: 5×10^9 ptc/ml; ×10: 5×10^{10} ptc/ml) for 48 h. After fixation, cells were subjected to immunofluorescence staining to probe MAP2 neuronal marker (A) and TUNEL assay to examine DNA fragmentation (B). In each group, images were taken from 5 to 6 wells to measure fluorescence intensity (for MAP2 staining) and fluorescent dot counts (for TUNEL assay). (C, D) Data were normalized to the control group and expressed as mean percentage values ± SEM. Significant differences between groups are indicated (**P < 0.01; ****P < 0.0001; one-way ANOVA followed by Tukey's multiple comparison test).

the lesioned side and contralateral (non-lesioned) brain hemispheres were collected for qRT-PCR analysis. Exo treatment significantly upregulated the expression of anti-apoptotic factors Bcl2 (Exo: 1.40 ± 0.07 vs Veh: 1.10 ± 0.06, *P* = 0.0471; Fig. 6A1) and Bcl-xL (Exo: 1.51 ± 0.07 vs Veh: 1.19 ± 0.06, *P* = 0.0001; Fig. 6A2) in the lesioned cortex. In contrast, Bcl2 (Exo: 1.275 ± 0.09 vs Veh: 1.261 ± 0.08, *P* = 0.9991; Fig. 6A1) and Bcl-xL (Exo: 1.08 ± 0.05 vs Veh: 1.11 ± 0.05, *P* = 0.981; Fig. 6A2) were not altered by Exos in the non-lesioned cortex.

WJ-MSC Exos Altered the Expression of Inflammatory Markers in the Stroke Brain

To investigate the effect of WJ-MSC-derived Exos on brain inflammation after cerebral ischemia, we examined the mRNA levels of pro-inflammatory cytokines (IL1β, IL6, TNFα), anti-inflammatory cytokines (IL10, TGFβ), and markers for M1 (CD86) and M2 (CD206) microglia in lesioned cortices. Exos significantly increased IL1β (28.53 ± 2.70 vs 15.00 ± 1.45, *P* < 0.0001; Fig. 6B1), IL6 (252.20 ± 34.50 vs 123.80 ± 16.55, *P* = 0.0002; Fig. 6B2), IL10 (21.73 ± 2.07 vs 12.18 ± 1.55, *P* < 0.0001; Fig. 6B4), TGFβ1 (13.12 ± 0.55 vs 10.38 ± 0.66, *P* = 0.0004; Fig. 6B5), and CD206 (28.91 ± 2.94 vs 17.96 ± 1.57, *P* = 0.0002; Fig. 6B11) in the lesioned cortex. There was no significant difference (Exo vs Veh) in the level of TNFα (5.68 ± 0.43 vs 4.66 ± 0.42, *P* = 0.102; Fig. 6B3) and CD86 (18.76 ± 0.99 vs 15.54 ± 1.41, *P* = 0.0567; Fig. 6B10) and

the ratios of IL1β/IL10 (1.42 ± 0.18 vs 1.42 ± 0.22, *P* > 0.9999; Fig. 6B6), IL6/IL10 (12.11 ± 1.45 vs 11.25 ± 1.73, *P* = 0.9515; Fig. 6B7), TNFα/IL10 (0.29 ± 0.04 vs 0.45 ± 0.06, *P* = 0.2498; Fig. 6B8), TNFα/TGFβ (0.43 ± 0.03 vs 0.45 ± 0.04, *P* = 0.9807; Fig. 6B9), and CD86/CD206 (0.73 ± 0.09 vs 0.89 ± 0.07, *P* = 0.426; Fig. 6B12) in the lesioned cortices between groups. These findings suggest that Exo transplants upregulated pro- and anti-inflammatory genes in the stroke brain.

WJ-MSC Exo Transplants Upregulated Protective Neurotrophic Factors in the Stroke Brain

We further investigated whether WJ-MSC Exos promoted the expression of neurotrophic factors after cerebral ischemia by analyzing the mRNA levels of three neurotrophic factors, BMP7, GDNF, and BDNF, in the cortex tissues of lesioned and non-lesioned brain hemispheres of stroke rats treated with Exos or saline (Fig. 6C1–C3). In the Veh group, the mRNA levels of BMP7 (3.42 ± 0.24 vs 1.39 ± 0.10, *P* = 0.0141; Fig. 6C1) and GDNF (15.90 ± 2.68 vs 0.85 ± 0.05, *P* < 0.0001; Fig. 6C2), but not BDNF (1.35 ± 0.19 vs 1.23 ± 0.11, *P* = 0.9072; Fig. 6C3) were significantly higher in the lesioned cortices than in the non-lesioned cortices, indicating that stroke increased the expression of BMP7 and GDNF. In the lesioned cortices, transplantation of Exos significantly increased BMP7 (5.71 ± 0.85 vs 3.42 ± 0.24, *P* = 0.0049; Fig. 6C1), GDNF (26.82 ± 2.37 vs 15.90± 2.68, *P* = 0.0006; Fig. 6C2), but not BDNF(Exo: 1.12 ± 0.12 vs
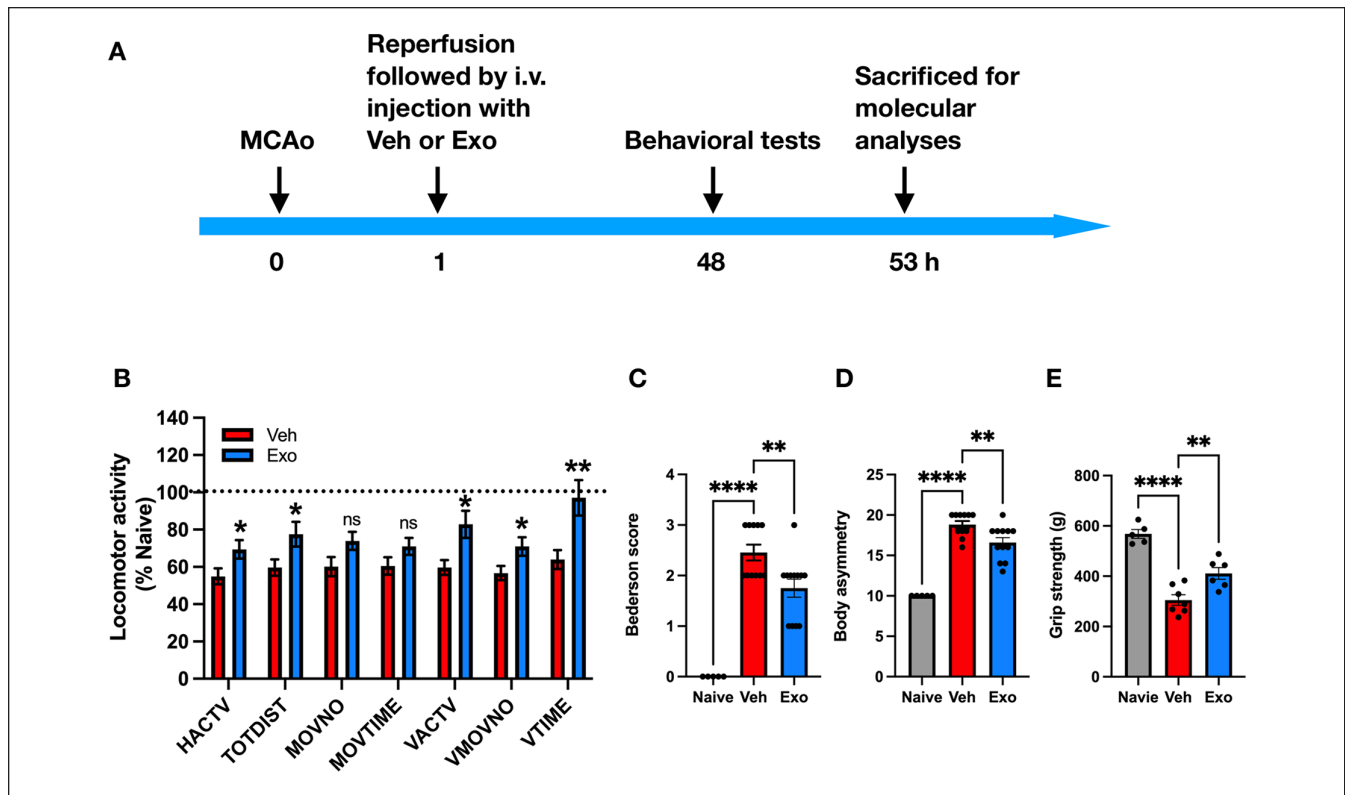
Figure 4. Exos improve locomotor activity and attenuate neurological deficits in ischemic stroke rats. (A) Experiment timeline. Adult rats underwent transient MCAo surgery by ligating the right distal MCA for 60 min. After reperfusion, rats were injected with saline (Veh; $n = 11$) or WJ-MSC exosomes (Exo; $n = 12$) via the tail vein. Two days later, naive rats ($n = 5$) and MCAo rats were examined for (B) locomotor activity for 2 h, (C) Bederson's neurological deficit score, (D) body asymmetry in 20 trials, and (E) grip strength of the left forelimb. Finally, animals were sacrificed, and brain tissues were collected for molecular analyses. Data were expressed as mean values $\pm$ SEM. Significant differences between groups are indicated (*$P < 0.05$; **$P < 0.01$; ****$P < 0.0001$, ns: not significant; B: Student's *t*-test, Exo vs Veh; C, D, E: one-way ANOVA followed by Dunnett's multiple comparison test).

Veh: 1.35 ± 0.19, $P = 0.5723$; Fig. 6C3). In contrast, GDNF, BDNF, BMP7 were not affected by Exo transplantation in the non-lesioned cortices. These findings suggest that the administration of WJ-MSC Exos further upregulated the expression of BMP7 and GDNF in the ischemic brain.

WJ-MSC Exos Contain Numerous Bioactive Molecules That May Contribute to the Beneficial Effects Observed in Stroke Rats Treated With Exos

It remains unclear whether these therapeutic outcomes arise from the direct action of the Exos or their paracrine effects. To investigate this, we further analyzed the molecular contents of WJ-MSC Exos, focusing on miRNAs, growth factors, and cytokines, which may be involved in neuroprotection, anti-inflammatory, or anti-apoptotic mechanisms. The miRNA profiles, determined by next-generation sequencing, were ranked based on total read counts (Fig. 7A). The top seven miRNAs accounted for 71.71% of the total 384 miRNAs identified in the Exos (Fig. 7B). Growth factors and cytokines were quantified

using multiplexed sandwich ELISA arrays. Among the 40 growth factors examined, 30 were detected and ranked by their abundance (Fig. 7C), with the top five comprising 89.72% of the total detected growth factors (Fig. 7D). Similarly, 38 of the 40 cytokines were identified and ranked (Fig. 7E), with the top seven representing 93.36% of the total cytokines in the Exos (Fig. 7F). The most prominent bioactive molecules—miRNAs (miR-16-5p, miR-126-3p, let-7f-5p, miR-125b-5p, let-7a-5p, let-7i-5p, miR-93-5p), growth factors (IGBP-4, BMP-4, BMP-7, IGFBP-2, FGF-4), and cytokines (TIMP-2, TIMP-1, ICAM-1, RANTES, G-CSF, IL-6sR, TNFRII)—have been previously reported to play neuroprotective roles in stroke models (as detailed in the Discussion section). Conversely, the minor components are unlikely to exert significant biological effects due to their low abundance. These findings suggest that the therapeutic effects of WJ-MSC Exos may, in part, be due to the major bioactive molecules they encapsulate.

Discussion

In this study, we characterized Exos isolated from human WJ-MSCs and investigated their potential in the treatment of

Figure 5. Exos reduce cerebral infarction in ischemic stroke rats. Adult rats underwent transient MCAo surgery by ligating the right distal MCA for 60 min. After reperfusion, rats were injected with saline (Veh; $n = 7$) or WJ-MSC exosomes (Exo; $n = 6$) via the tail vein. (A) Two days after MCAo, rats were sacrificed, and brains were sliced for TTC staining to examine the volume of infarct areas (white patch). Scale bar: 10 mm. (B) The integrated infarction volume was measured from scanned images of brain slides. Data were expressed as mean values $\pm$ SEM. Significant differences between groups are indicated ($*P < 0.05$; Student's t-test).

cerebral ischemic stroke. We found that systemic transplantation of Exos from human WJ-MSCs significantly reduced brain infarction, lowered Bederson's neurological scores and body asymmetry, and increased locomotor activity and forearm grip strength in stroke rats. Exo treatment also led to increased expression of neurotrophic factors (BMP7, GDNF) and anti-apoptotic factors (Bcl2, Bcl-xL) in the brain tissue damaged by MCAo. We also revealed that Exo administration significantly reduces glutamate-mediated neuronal loss and apoptosis in PNC cultures. Our data support the idea that early post-treatment with WJ-MSC Exos protects against neuronal damage and improves functional recovery in the brain affected by stroke.

Cells isolated from Wharton's jelly of hUCs exhibit morphology similar to that of fibroblasts and express MSC surface markers (CD73, CD90, CD105), but not the hematopoietic stem cell marker (CD34). This observation aligns with previous studies on the characterization of human WJ-MSCs[43–45]. Vesicles purified from the conditioned medium of human WJ-MSC cultures are spherical, ranging in size from 45 to 180 nm, and display typical Exo markers (CD9, CD63, CD81, HSP70, TSG101) without the presence of endoplasmic reticulum marker (Calnexin), consistent with Exo characterization standards[30,55]. These findings confirm that human WJ-MSCs were successfully isolated from hUCs, and the Exos collected for this study were purified from WJ-MSCs without contamination of endoplasmic reticulum components.

The protective effect of WJ-MSC Exos was first examined in PNC cultures. A high dose (100 μM) of glutamate was used to generate neurodegeneration as previously described[56,57] and to simulate overflow of concentrated glutamate during cerebral ischemia[58]. Glutamate significantly reduced MAP2 immunoreactivity and increased TUNEL activity. Both responses were significantly mitigated by WJ-MSC Exos, indicating that these Exos attenuated glutamate-induced apoptosis and neuronal loss. This neuroprotective effect is

further supported by *in vivo* experiments, where systemic administration of WJ-MSC Exos increased the expression of anti-apoptotic factors Bcl-2 and Bcl-xL in the lesioned brain tissues. These data suggest that WJ-MSC Exos induced protection through the suppression of apoptosis.

Comparatively, Exos derived from other sources also processed anti-apoptotic properties in stroke brains. For example, Exos from rat bone marrow MSCs inhibit apoptosis by reducing KDM6B expression and reduce neuronal damage in stroke rats[59]. Exos from mouse bone marrow MSCs inhibit apoptosis by suppressing CDK6 in stoke mice[60]. Exos derived from rat bone marrow MSCs downregulated caspase-8-dependent apoptosis in oxygen-glucose-deprived cultures of oligodendrocytes[25]. While these findings highlight the therapeutic potential of MSC-derived Exos through anti-apoptosis in mitigating neuronal damage and promoting recovery in ischemic stroke, further investigation is required to determine the anti-apoptotic mechanisms of WJ-MSC Exos.

Numerous studies have demonstrated that the use of MSCs can enhance neurological function recovery in stroke animals. This benefit is accomplished by promoting the growth of new blood vessels and nerve cells while also reducing inflammation and cell death[61–65]. Notably, evidence suggests that the beneficial effects of MSCs are partly mediated by the secretion of Exos rather than direct cell replacement[12,66,67]. Recent investigations utilizing Exos derived from MSCs obtained from various tissues, such as rat bone marrow, rat adipose, human bone marrow, and hUC blood, have shown promising results in improving neurological function recovery in animal models of ischemic stroke[12,22,68,69]. Furthermore, studies have demonstrated that direct injection of hUC-MSCs into the brain or systemic administration can reduce brain injury and neurological deficits in rodent stroke models[9,70–72]. Therefore, Exos derived from hUC-MSCs may have similar effects in protecting neurons and enhancing functional recovery in the rat model of ischemic stroke.
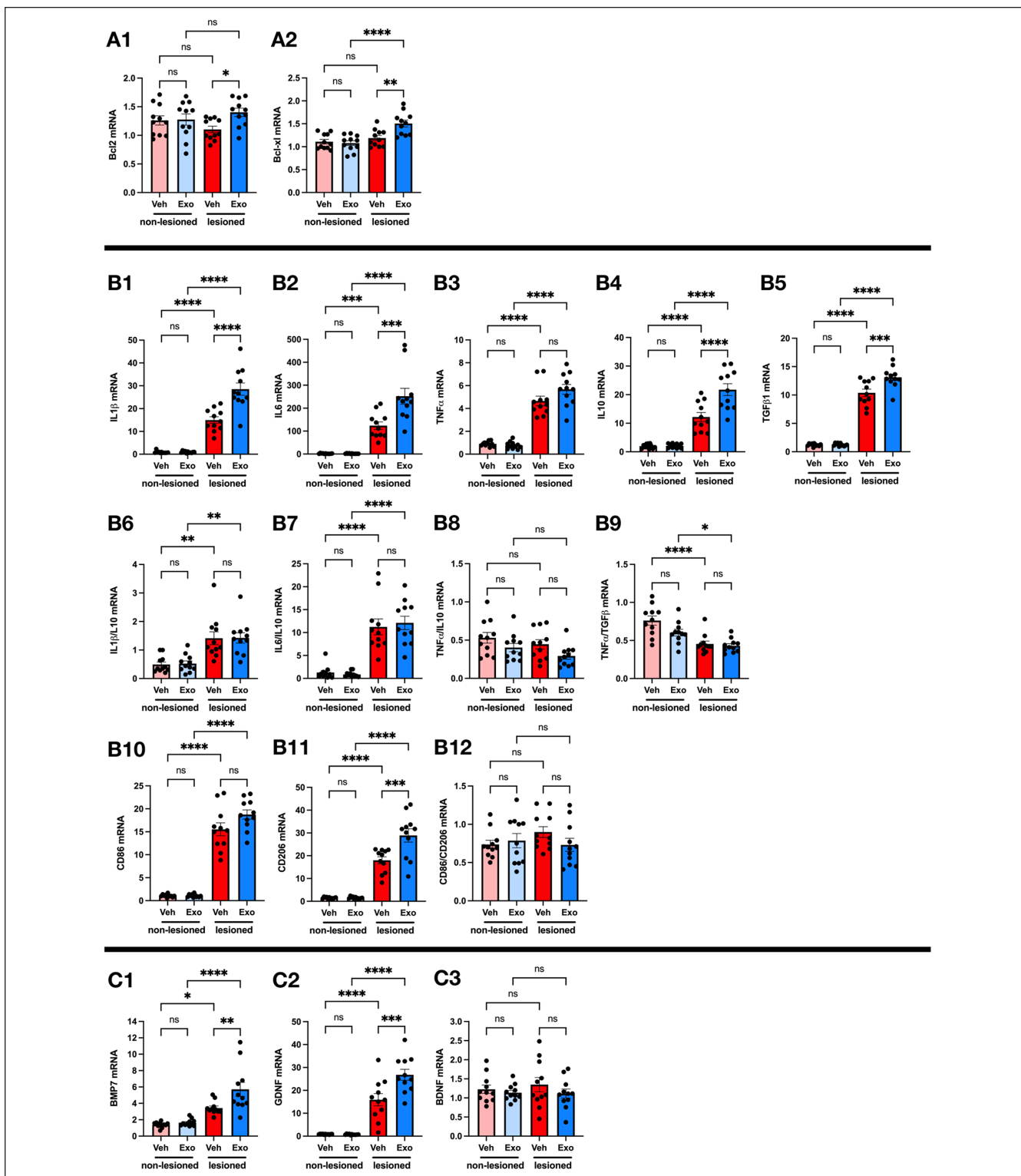
Figure 6. Effects of Exo treatment on the expression of apoptotic, inflammatory, and neurotrophic factors in the brain of ischemic stroke rats. Adult rats were subjected to transient MCAo surgery by ligating the right distal MCA for 60 min. After reperfusion, rats were injected with saline (Veh; $n = 11$) or WJ-MSC exosomes (Exo; $n = 11$) via the tail vein. Two days after MCAo, the cortex tissues of lesioned and non-lesioned brain sides were collected for qRT-PCR to examine the mRNA levels of apoptotic (Bcl2, Bcl-xl; A1, A2), inflammatory (CD86, CD206, IL1β, IL6, IL10, TGFβ1, and TNFα; B1–B12), and neurotrophic factors (BMP7, GDNF, and BDNF; C1, C2, C3). The mRNA level of examined genes was normalized to that of GAPDH and measured as fold or ratio changes. Data are expressed as mean values ± SEM, and significant differences between groups are indicated (*$P < 0.05$; **$P < 0.01$; ***$P < 0.001$; ****$P < 0.0001$, ns: not significant; one-way ANOVA followed by Tukey's multiple comparison test).
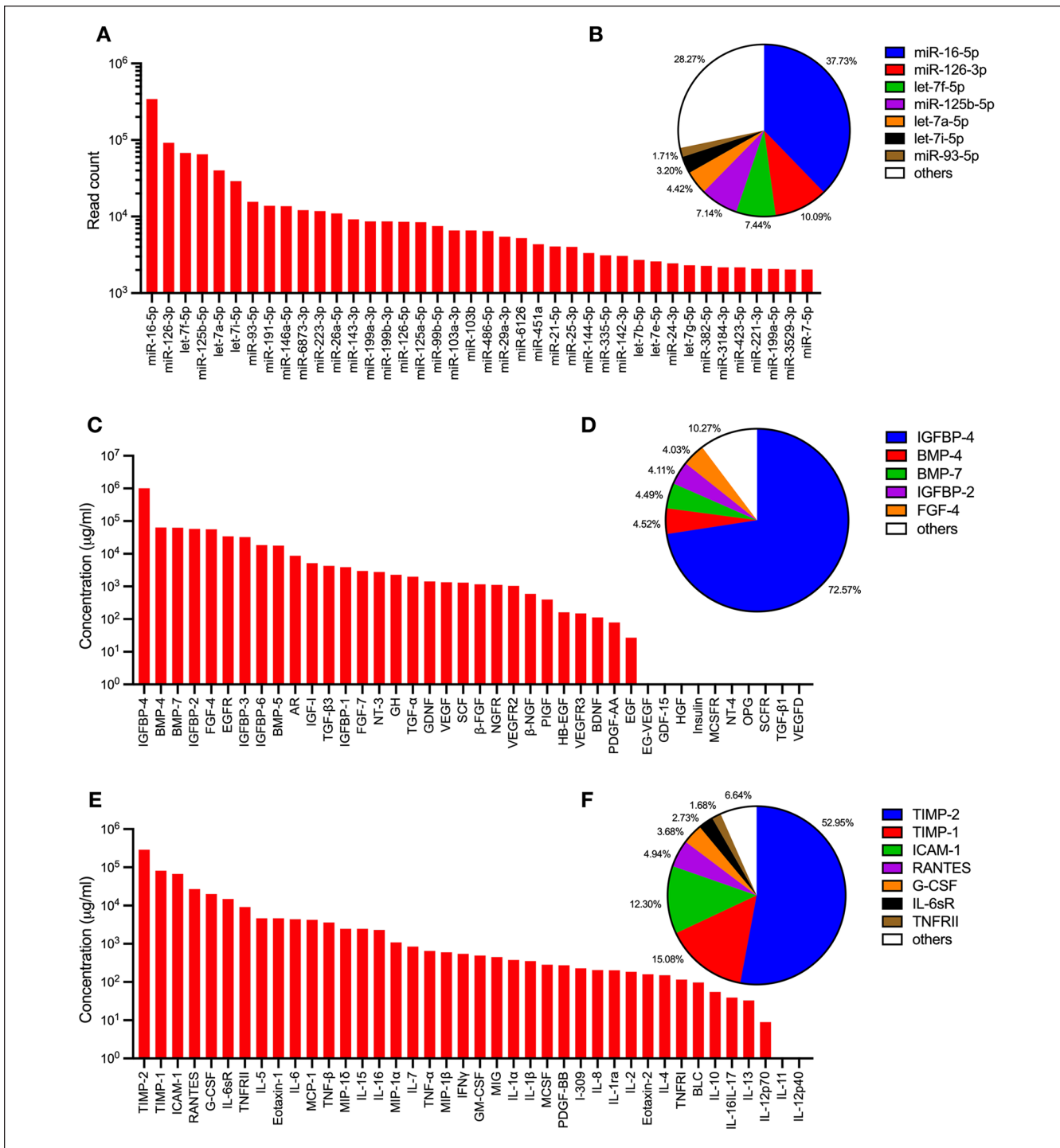
Figure 7. Bioactive molecule profiles in Exos. The miRNA content of WJ-MSC Exos was analyzed via next-generation sequencing. The total read counts of the top 40 miRNAs are displayed (A), with the top seven miRNAs accounting for 71.71% of the total 384 miRNAs identified in the Exos (B). Growth factors and cytokines present in the Exos were quantified using multiplexed sandwich ELISA-based arrays. Of the 40 growth factors analyzed, 30 were detected (C), with the top five comprising 89.72% of the total detected growth factors (D). In addition, 38 of the 40 cytokines were identified (E), with the top seven representing 93.36% of the total cytokines detected in the Exos (F).

The beneficial effects of Exo treatment on protection and repair in cerebral ischemic stroke rats are highlighted by its ability to enhance the expression of essential neurotrophic factors, such as BMP7 and GDNF. BMP7 possesses neurogenic and neuroprotective properties, promoting neuronal differentiation and dendritic growth, while GDNF exerts

potent trophic effects on various types of neurons, facilitating cell survival and axonal outgrowth[73–77]. After stroke-induced injury, these neurotrophic factors are upregulated, contributing substantially to promoting neuronal survival, regeneration, and functional recovery[78–80]. By enhancing the upregulation of BMP7 and GDNF, WJ-MSC-derived Exos may create a suitable microenvironment for neurogenesis and synaptic plasticity within the injured brain tissue, ultimately restoring neurological function. However, the expression of BDNF was not altered in the stroke rats after Exo treatment. Although BDNF is a well-known neurotrophic factor implicated in neuronal survival, neurogenesis, and synaptic plasticity[81–84], its unchanged expression suggests that the beneficial effects of Exo treatment in ischemic stroke rats may not be attributed to the action of BDNF.

MSC-derived Exos may prevent or reverse neuronal damage by delivering bioactive molecules such as miRNAs and proteins that regulate critical signaling pathways involved in neuronal repair and functional recovery[85–87]. Notably, seven miRNAs—miR-16-5p, miR-126-3p, let-7f-5p, miR-125b-5p, let-7a-5p, let-7i-5p, and miR-93-5p—make up 71.71% of the 384 miRNAs identified in WJ-MSC Exos, each potentially contributing to stroke recovery. miR-16-5p, the most abundant, has been shown to promote the survival of cortical neurons and reduce apoptosis by targeting AKT3 in an oxygen-glucose deprivation model of cerebral ischemia[88]. Members of the let-7 miRNA family offer neuroprotection in cerebral ischemic stroke by regulating proteins involved in inflammatory pathways, including the SMAD3/TGFβ axis within the central nervous system[89]. In addition, overexpression of miR-126-5p has been shown to protect the BBB and reduce pro-inflammatory cytokines in a mouse model of MCAo[90]. miR-125b-5p and miR-93-5p are involved in modulating excitotoxicity and oxidative stress, respectively, after ischemic stroke[91,92].

Among the growth factors present in WJ-MSC Exos, five (IGFBP-4, BMP-4, BMP-7, IGFBP-2, and FGF-4) account for 89.72% of the total identified and may contribute to stroke recovery. IGFBP-4, the most abundant growth factor, has been shown to promote neuronal survival and neurite outgrowth following cerebral ischemia[93]. BMP-7 and FGF-4 have been linked to neuroregeneration by stimulating the proliferation of neuronal precursors[94,95], while BMP-4 has been shown to support neuronal stem cell proliferation and cell survival in an *in vitro* model of oxygen-glucose deprivation[96].

In addition, seven cytokines—TIMP-2, TIMP-1, ICAM-1, RANTES, G-CSF, IL-6sR, and TNFRII—representing 93.36% of the total cytokines in WJ-MSC Exos may also contribute to recovery after stroke. TIMP-2 and TIMP-1, the most abundant, reduce ischemic damage by modulating matrix metalloproteinase (MMP) activity and activating intracellular kinase-dependent pathways[97,98]. ICAM-1 in Exos may help decrease infarct size by preventing leukocyte migration into the brain parenchyma[99]. While RANTES is typically pro-inflammatory, it may promote cell survival and

neurotrophic factor upregulation by activating Akt and Erk1/2 pathways in peri-infarct areas[100]. G-CSF has been shown to reduce lesion size, improve motor function, and lower mortality in transient ischemic stroke, likely by acting on its receptors in the ischemic penumbra[101]. Last, IL-6sR and TNFRII serve as buffers to prevent overstimulation from IL6 and TNFα, two pro-inflammatory cytokines involved in ischemic brain injury[102,103]. These improvements highlight the potential of Exo therapy as a multifaceted and effective strategy for reducing neurological deficits caused by ischemic stroke.

We previously demonstrated the intracerebral transplantation of human WJ-MSCs reduced brain infarction and improved motor functions in stroke rats[19]. The protective effect was associated with a strong anti-inflammatory effect in the lesioned cortex. In contrast, in this study, we found that human WJ-MSC Exos given intravenously did not process strong anti-inflammatory function. Exo treatment resulted in an increased expression of anti-inflammatory cytokines (IL10, TGFβ) and an M2 microglia marker (CD206) in the lesioned cortices. At the same time, there was an upregulation of pro-inflammatory cytokines (IL1β, IL6, TNFα) and an M1 microglia marker (CD86). These results indicate that Exos triggered pro- and anti-inflammatory pathways but did not skew to either pathway, as the ratios of pro/anti-inflammation cytokines and microglia polarization (M1/M2) were not altered. The differential inflammatory responses between WJ-MSCs and WJ-MSC Exos may be attributed to the route, dose, or timing of transplantation, highlighting the intricate nature of our research. Further investigation is necessary to understand the specific mechanisms by which Exos orchestrate this delicate balance.

Exo treatment for ischemic stroke offers several advantages over cell-based therapies that use MSCs. One major advantage is avoiding potential safety concerns associated with cell transplantation, such as immune rejection, tumorigenesis, and embolism formation[104–106]. Exos can be administered via various non-invasive routes, such as intravenous injection, intranasal delivery, and intra-arterial infusion[12,107,108]. Therefore, Exo therapy is conducted through more accessible administration routes than invasive procedures required for cell transplantation, reducing procedural risks and costs and enhancing patient compliance. In addition, Exos possess unique properties that allow them to traverse biological barriers, including the BBB, enabling targeted delivery to the site of injury in the brain[109,110]. Exos are extracellular vesicles secreted by MSCs, containing bioactive molecules, including proteins, nucleic acids, and lipids, that modulate various cellular processes involved in neuroprotection, angiogenesis, neurogenesis, and anti-inflammatory responses. Exo treatment could be a promising and versatile therapeutic strategy for ischemic stroke, with the potential to overcome many limitations associated with cell-based therapies.

To bridge our present findings to clinical applications, we need to address several critical aspects. (1) Delivery Routes: In

our study, we administered Exos systemically via intravenous injection, which is feasible for clinical use. However, alternative routes such as intra-arterial delivery or local administration to the ischemic brain region may offer more precise targeting, minimizing off-target effects and potentially improving outcomes[111,112]. A detailed evaluation of the pros and cons of these methods is necessary to determine the most effective delivery strategy for human applications. (2) Dosage: Establishing an optimal dose for clinical application is crucial[113]. Our study demonstrated efficacy with a specific dose in rats, but human trials would need to consider dose scaling based on body size and stroke severity. Dose-response studies will help refine therapeutic regimens to ensure both efficacy and safety for patients[114]. (3) Timing of Administration: The timing of Exo treatment is another critical aspect. Our data suggest that early post-stroke intervention is beneficial, but in clinical settings, stroke patients may present at different times after onset. Exploring how treatment windows affect outcomes and understanding the balance between early and delayed interventions are essential for maximizing recovery in diverse clinical scenarios[115]. (4) Patient Selection: Not all stroke patients will respond equally to Exo therapy. Potential selection criteria such as stroke type, severity, and patient-specific factors (e.g., age, comorbidities, genetic predispositions) could influence treatment efficacy[116,117]. Identifying reliable biomarkers to predict responsiveness could help patient selection and improve treatment outcomes[118]. (5) Safety and Regulatory Considerations: Safety issues such as immune responses, potential off-target effects, and long-term safety in patients must be carefully evaluated. Current clinical guidelines for cell-based therapies may be adapted to address the regulatory challenges regarding the use of MSC-derived Exos as therapeutic agents[119]. By addressing these considerations in the clinical translation of WJ-MSC Exo therapy, we aim to provide a clearer roadmap for future clinical trials and potential therapeutic use in stroke patients.

Despite the promising findings of this study, further investigation is needed to fully understand the therapeutic potential of Exos derived from WJ-MSCs in treating cerebral ischemic stroke. First, this study did not assess whether the administered Exos reached the damaged brain region, which is crucial for validating their direct therapeutic effects. Second, the impact of different Exo dosages on treatment outcomes was not explored, making it uncertain whether there is an optimal dose or whether the observed benefits are dose-dependent. Third, the long-term effects of Exo treatment were not evaluated, leaving it unclear whether the improvements in brain damage and neurological outcomes are sustained over time or whether additional treatments are required for lasting therapeutic benefits. In addition, this study lacked a detailed immunohistochemistry analysis of neuronal pathology in the penumbra region, the peri-infarct area critical for behavioral recovery after stroke[120–122]. Examining these aspects could provide detailed insights into the cellular and molecular changes induced by Exo treatment. These limitations need to be addressed in future

research to establish the efficacy, optimal administration protocols, and long-term sustainability of WJ-MSC-derived Exos as a treatment for cerebral ischemic stroke.

In conclusion, we demonstrate that early intravenous administration of Exos from human WJ-MSCs can significantly enhance functional recovery and mitigate brain damage in the stroke animal model. Given the non-invasive nature of this therapeutic approach, our study not only offers promising insights but also opens up exciting possibilities for potential clinical applications in stroke treatment.

Author Contributions

Conceptualization: YHC
Data curation: YSC, KJW, SJY, KLW, CYH, YSC, KYC, YSW, EKB, TWH, SHL, CHL, SCH, YHC
Formal analysis: YSC, KJW, YSW, YHC
Funding acquisition: YHC
Investigation: YSC, KJW, SJY, KLW, CYH, YSC, KYC, YSW, EKB, TWH, SHL, CHL, SCH
Methodology: YSC, KJW, SJY, CYH, YSC, KYC, YSW, EKB, YHC
Project administration: YHC
Resources: SJY, KLW, SCH, YW, YHC
Supervision: YW, YHC
Validation: YSC, KJW, CYH, YSW, EKB, YHC
Visualization: YHC
Writing-original draft: YHC
Writing-review & editing: YW, YHC
All authors read and approved the final manuscript.

Ethical Approval

This study was conducted in accordance with the Declaration of Helsinki and approved by the Institutional Review Board (IRB) of Fu Jen Catholic University (approval no. C111157) on July 18, 2023. The Institutional Animal Care and Use Committee of the National Health Research Institutes in Taiwan approved the experimental procedures used in this study (approval no. NHRI-IACUC-112034-A) on March 21, 2023.

Statement of Human and Animal Rights

All animal housing and experiments were conducted in strict accordance with the institutional Guidelines for the Care and Use of Laboratory Animals at the National Health Research Institutes.

Statement of Informed Consent

Written informed consent for donating discarded umbilical cords in this study was obtained from the donors before participating.

Data Availability

All relevant data included in the paper are available from the corresponding author upon reasonable request.

ORCID iDs

Yu-Sung Chiu https://orcid.org/0000-0002-6429-5878
Yun-Hsiang Chen https://orcid.org/0000-0002-2439-1080

References

1. Lloyd-Jones D, Adams R, Carnethon M, De Simone G, Ferguson TB, Flegal K, Ford E, Furie K, Go A, Greenlund K, Haase N, et al. Heart disease and stroke statistics—2009 update: a report from the American Heart Association Statistics Committee and Stroke Statistics Subcommittee. Circulation. 2009;119(3):480–86.

2. Lackland DT, Roccella EJ, Deutsch AF, Fornage M, George MG, Howard G, Kissela BM, Kittner SJ, Lichtman JH, Lisabeth LD, Schwamm LH, et al. Factors influencing the decline in stroke mortality: a statement from the American Heart Association/American Stroke Association. Stroke. 2014;45(1):315–53.

3. Benjamin EJ, Muntner P, Alonso A, Bittencourt MS, Callaway CW, Carson AP, Chamberlain AM, Chang AR, Cheng S, Das SR, Delling FN, et al. Heart disease and stroke statistics-2019 update: a report from the American Heart Association. Circulation. 2019;139(10):e56–528.

4. Prentice H, Modi JP, Wu JY. Mechanisms of neuronal protection against excitotoxicity, endoplasmic reticulum stress, and mitochondrial dysfunction in stroke and neurodegenerative diseases. Oxid Med Cell Longev. 2015;2015:964518.

5. Kalogeris T, Baines CP, Krenz M, Korthuis RJ. Ischemia/reperfusion. Compr Physiol. 2016;7(1):113–70.

6. Zerna C, Thomalla G, Campbell BCV, Rha JH, Hill MD. Current practice and future directions in the diagnosis and acute treatment of ischaemic stroke. Lancet. 2018;392(10154):1247–56.

7. Vu Q, Xie K, Eckert M, Zhao W, Cramer SC. Meta-analysis of preclinical studies of mesenchymal stromal cells for ischemic stroke. Neurology. 2014;82(14):1277–86.

8. Lee SH, Jin KS, Bang OY, Kim BJ, Park SJ, Lee NH, Yoo KH, Koo HH, Sung KW. Differential migration of mesenchymal stem cells to ischemic regions after middle cerebral artery occlusion in rats. PLoS ONE. 2015;10(8):e0134920.

9. Wu KJ, Yu SJ, Chiang CW, Cho KH, Lee YW, Yen BL, Kuo LW, Wang Y. Transplantation of human placenta-derived multipotent stem cells reduces ischemic brain injury in adult rats. Cell Transplant. 2015;24(3):459–70.

10. Uccelli A, Moretta L, Pistoia V. Mesenchymal stem cells in health and disease. Nat Rev Immunol. 2008;8(9):726–36.

11. Hu J, Zhang L, Wang N, Ding R, Cui S, Zhu F, Xie Y, Sun X, Wu D, Hong Q, Li Q, et al. Mesenchymal stem cells attenuate ischemic acute kidney injury by inducing regulatory T cells through splenocyte interactions. Kidney Int. 2013;84(3):521–31.

12. Xin H, Li Y, Cui Y, Yang JJ, Zhang ZG, Chopp M. Systemic administration of exosomes released from mesenchymal stromal cells promote functional recovery and neurovascular plasticity after stroke in rats. J Cereb Blood Flow Metab. 2013;33(11):1711–15.

13. Bronckaers A, Hilkens P, Martens W, Gervois P, Ratajczak J, Struys T, Lambrichts I. Mesenchymal stem/stromal cells as a pharmacological and therapeutic approach to accelerate angiogenesis. Pharmacol Ther. 2014;143(2):181–96.

14. Dulamea AO. The potential use of mesenchymal stem cells in stroke therapy–from bench to bedside. J Neurol Sci. 2015;352(1–2):1–11.

15. Dennis JE, Carbillet JP, Caplan AI, Charbord P. The STRO-1+ marrow cell population is multipotential. Cells Tissues Organs. 2002;170(2–3):73–82.

16. Visweswaran M, Pohl S, Arfuso F, Newsholme P, Dilley R, Pervaiz S, Dharmarajan A. Multi—lineage differentiation of mesenchymal stem cells—to Wnt, or not Wnt. Int J Biochem Cell Biol. 2015;68:139–47.

17. Can A, Karahuseyinoglu S. Concise review: human umbilical cord stroma with regard to the source of fetus-derived stem cells. Stem Cells. 2007;25(11):2886–95.

18. Beeravolu N, McKee C, Alamri A, Mikhael S, Brown C, Perez-Cruet M, Chaudhry GR. Isolation and characterization of mesenchymal stromal cells from human umbilical cord and fetal placenta. J Vis Exp. 2017(122):55224.

19. Wu KJ, Yu SJ, Chiang CW, Lee YW, Yen BL, Tseng PC, Hsu CS, Kuo LW, Wang Y. Neuroprotective action of human Wharton's Jelly-derived mesenchymal stromal cell transplants in a rodent model of stroke. Cell Transplant. 2018;27(11):1603–12.

20. Seyedaghamiri F, Salimi L, Ghaznavi D, Sokullu E, Rahbarghazi R. Exosomes-based therapy of stroke, an emerging approach toward recovery. Cell Commun Signal. 2022;20(1):110.

21. Xiong Y, Song J, Huang X, Pan Z, Goldbrunner R, Stavrinou L, Lin S, Hu W, Zheng F, Stavrinou P. Exosomes derived from mesenchymal stem cells: novel effects in the treatment of ischemic stroke. Front Neurosci. 2022;16:899887.

22. Jiang M, Wang H, Jin M, Yang X, Ji H, Jiang Y, Zhang H, Wu F, Wu G, Lai X, Cai L, et al. Exosomes from MiR-30d-5p-ADSCs reverse acute ischemic stroke-induced, autophagy-mediated brain injury by promoting M2 microglial/macrophage polarization. Cell Physiol Biochem. 2018;47(2):864–78.

23. Zhao Y, Gan Y, Xu G, Hua K, Liu D. Exosomes from MSCs overexpressing microRNA-223-3p attenuate cerebral ischemia through inhibiting microglial M1 polarization mediated inflammation. Life Sci. 2020;260:118403.

24. Li H, Luo Y, Liu P, Liu P, Hua W, Zhang Y, Zhang L, Li Z, Xing P, Zhang Y, Hong B, et al. Exosomes containing miR-451a

is involved in the protective effect of cerebral ischemic precon-ditioning against cerebral ischemia and reperfusion injury. CNS Neurosci Ther. 2021;27(5):564–76.

25. Xiao Y, Geng F, Wang G, Li X, Zhu J, Zhu W. Bone marrow-derived mesenchymal stem cells-derived exosomes prevent oligodendrocyte apoptosis through exosomal miR-134 by tar-geting caspase-8. J Cell Biochem. 2019;120(2):2109–18.

26. Yang Y, Cai Y, Zhang Y, Liu J, Xu Z. Exosomes secreted by adipose-derived stem cells contribute to angiogenesis of brain microvascular endothelial cells following oxygen-glucose deprivation in vitro through MicroRNA-181b/TRPM7 axis. J Mol Neurosci. 2018;65(1):74–83.

27. Xin H, Liu Z, Buller B, Li Y, Golembieski W, Gan X, Wang F, Lu M, Ali MM, Zhang ZG, Chopp M. MiR-17-92 enriched exosomes derived from multipotent mesenchymal stromal cells enhance axon-myelin remodeling and motor electrophysi-ological recovery after stroke. J Cereb Blood Flow Metab. 2021;41(5):1131–44.

28. van Niel G, D'Angelo G, Raposo G. Shedding light on the cell biology of extracellular vesicles. Nat Rev Mol Cell Biol. 2018;19(4):213–28.

29. Jafari D, Malih S, Eslami SS, Jafari R, Darzi L, Tarighi P, Samadikuchaksaraei A. The relationship between molecular content of mesenchymal stem cells derived exosomes and their potentials: opening the way for exosomes based therapeutics. Biochimie. 2019;165:76–89.

30. Colombo M, Raposo G, Théry C. Biogenesis, secretion, and intercellular interactions of exosomes and other extracellular vesicles. Annu Rev Cell Dev Biol. 2014;30:255–89.

31. Alvarez-Erviti L, Seow Y, Yin H, Betts C, Lakhal S, Wood MJ. Delivery of siRNA to the mouse brain by systemic injec-tion of targeted exosomes. Nat Biotechnol. 2011;29(4):341–45.

32. Zhuang X, Xiang X, Grizzle W, Sun D, Zhang S, Axtell RC, Ju S, Mu J, Zhang L, Steinman L, Miller D, et al. Treatment of brain inflammatory diseases by delivering exosome encap-sulated anti-inflammatory drugs from the nasal region to the brain. Mol Ther. 2011;19(10):1769–79.

33. Haney MJ, Klyachko NL, Zhao Y, Gupta R, Plotnikova EG, He Z, Patel T, Piroyan A, Sokolsky M, Kabanov AV, Batrakova EV. Exosomes as drug delivery vehicles for Parkinson's dis-ease therapy. J Control Release. 2015;207:18–30.

34. Sterzenbach U, Putz U, Low LH, Silke J, Tan SS, Howitt J. Engineered exosomes as vehicles for biologically active pro-teins. Mol Ther. 2017;25(6):1269–78.

35. Chen YH, Wu KL, Chen CH. Methamphetamine reduces human influenza A virus replication. PLoS ONE. 2012;7(11):e48335.

36. Chen YH, Yu SJ, Wu KJ, Wang YS, Tsai HM, Liao LW, Chen S, Hsieh W, Chen H, Hsu SC, Chen ML, et al. Downregulation of α-synuclein protein levels by an intracellular single-chain antibody. J Parkinsons Dis. 2020;10(2):573–90.

37. Festing MF, Altman DG. Guidelines for the design and statis-tical analysis of experiments using laboratory animals. Ilar J. 2002;43(4):244–58.

38. Borlongan CV, Hida H, Nishino H. Early assessment of motor dysfunctions aids in successful occlusion of the middle cere-bral artery. Neuroreport. 1998;9(16):3615–21.

39. Airavaara M, Shen H, Kuo CC, Peränen J, Saarma M, Hoffer B, Wang Y. Mesencephalic astrocyte-derived neurotrophic factor reduces ischemic brain injury and promotes behavioral recovery in rats. J Comp Neurol. 2009;515(1):116–24.

40. Bederson JB, Pitts LH, Tsuji M, Nishimura MC, Davis RL, Bartkowski H. Rat middle cerebral artery occlusion: evaluation of the model and development of a neurologic examination. Stroke. 1986;17(3):472–76.

41. Chiu YS, Wu KJ, Yu SJ, Wu KL, Wang YS, Lin J, Chu CY, Chen S, Chen H, Hsu SC, Wang Y, et al. Peptide immunization against the C-terminal of alpha-synuclein reduces locomotor activity in mice overexpressing alpha-synuclein. PLoS ONE. 2023;18(9):e0291927.

42. Livak KJ, Schmittgen TD. Analysis of relative gene expres-sion data using real-time quantitative PCR and the 2(-Delta Delta C(T)) Method. Methods. 2001;25(4):402–408.

43. Chang YH, Wu KC, Liu HW, Chu TY, Ding DC. Human umbilical cord-derived mesenchymal stem cells reduce mono-sodium iodoacetate-induced apoptosis in cartilage. Ci Ji Yi Xue Za Zhi. 2018;30(2):71–80.

44. Ahmadvand Koohsari S, Absalan A, Azadi D. Human umbili-cal cord mesenchymal stem cell-derived extracellular vesicles attenuate experimental autoimmune encephalomyelitis via regulating pro and anti-inflammatory cytokines. Sci Rep. 2021;11(1):11658.

45. Semenova E, Grudniak MP, Machaj EK, Bocian K, Chroscinska-Krawczyk M, Trochonowicz M, Stepaniec IM, Murzyn M, Zagorska KE, Boruczkowski D, Kolanowski TJ, et al. Mesenchymal stromal cells from different parts of umbilical cord: approach to comparison & characteristics. Stem Cell Rev Rep. 2021;17(5):1780–95.

46. Enderle D, Spiel A, Coticchia CM, Berghoff E, Mueller R, Schlumpberger M, Sprenger-Haussels M, Shaffer JM, Lader E, Skog J, Noerholm M. Characterization of RNA from exo-somes and other extracellular vesicles isolated by a novel spin column-based method. PLoS ONE. 2015;10(8):e0136133.

47. Watson DC, Yung BC, Bergamaschi C, Chowdhury B, Bear J, Stellas D, Morales-Kastresana A, Jones JC, Felber BK, Chen X, Pavlakis GN. Scalable, cGMP-compatible purifica-tion of extracellular vesicles carrying bioactive human het-erodimeric IL-15/lactadherin complexes. J Extracell Vesicles. 2018;7(1):1442088.

48. Sunderland N, Skroblin P, Barwari T, Huntley RP, Lu R, Joshi A, Lovering RC, Mayr M. MicroRNA biomarkers and platelet reactivity: the clot thickens. Circ Res. 2017;120(2):418–35.

49. Bordin A, Chirivì M, Pagano F, Milan M, Iuliano M, Scaccia E, Fortunato O, Mangino G, Dhori X, De Marinis E, D'Amico A, et al. Human platelet lysate-derived extracellular vesicles enhance angiogenesis through miR-126. Cell Prolif. 2022; 55(11):e13312.

50. Shen H, Kuo CC, Chou J, Delvolve A, Jackson SN, Post J, Woods AS, Hoffer BJ, Wang Y, Harvey BK. Astaxanthin reduces ischemic brain injury in adult rats. FASEB J. 2009;23(6):1958–68.

51. Harvey BK, Airavaara M, Hinzman J, Wires EM, Chiocco MJ, Howard DB, Shen H, Gerhardt G, Hoffer BJ, Wang Y. Targeted over-expression of glutamate transporter 1 (GLT-1) reduces ischemic brain injury in a rat model of stroke. PLoS ONE. 2011;6(8):e22135.

52. Wang Y, Harvey BK. Reducing excitoxicity with glutamate transporter-1 to treat stroke. Brain Circ. 2016;2(3):118–20.

53. Wu KJ, Chen YH, Bae EK, Song Y, Min W, Yu SJ. Human Milk oligosaccharide 2'-Fucosyllactose Reduces neurodegen-eration in stroke brain. Transl Stroke Res. 2020;11(5):1001–11.

54. Wu KJ, Wang YS, Hung TW, Bae EK, Chen YH, Kim CK, Yoo DW, Kim GS, Yu SJ. Herbal formula PM012 induces neuroprotection in stroke brain. PLoS ONE. 2023;18(2):e0281421.

55. Théry C, Amigorena S, Raposo G, Clayton A. Isolation and characterization of exosomes from cell culture supernatants and biological fluids. Curr Protoc Cell Biol. 2006; Chapter 3:Unit 3.22.

56. Choi DW, Maulucci-Gedde M, Kriegstein AR. Glutamate neurotoxicity in cortical cell culture. J Neurosci. 1987;7(2):357–68.

57. Wu KJ, Yu SJ, Shia KS, Wu CH, Song JS, Kuan HH, Yeh KC, Chen CT, Bae E, Wang Y. A novel CXCR4 antagonist CX549 induces neuroprotection in stroke brain. Cell Transplant. 2017;26(4):571–83.

58. Shen H, Chen GJ, Harvey BK, Bickford PC, Wang Y. Inosine reduces ischemic brain injury in rats. Stroke. 2005;36(3):654–59.

59. Zhang Y, Liu J, Su M, Wang X, Xie C. Exosomal microRNA-22-3p alleviates cerebral ischemic injury by modulating KDM6B/BMP2/BMF axis. Stem Cell Res Ther. 2021;12(1):111.

60. Cheng C, Chen X, Wang Y, Cheng W, Zuo X, Tang W, Huang W. MSCs-derived exosomes attenuate ischemia-reperfusion brain injury and inhibit microglia apoptosis might via exosomal miR-26a-5p mediated suppression of CDK6. Mol Med. 2021;27(1):67.

61. Chen J, Li Y, Katakowski M, Chen X, Wang L, Lu D, Lu M, Gautam SC, Chopp M. Intravenous bone marrow stromal cell therapy reduces apoptosis and promotes endogenous cell proliferation after stroke in female rat. J Neurosci Res. 2003;73(6):778–86.

62. Yoo SW, Kim SS, Lee SY, Lee HS, Kim HS, Lee YD, Suh-Kim H. Mesenchymal stem cells promote proliferation of endogenous neural stem cells and survival of newborn cells in a rat stroke model. Exp Mol Med. 2008;40(4):387–97.

63. Zhang ZG, Chopp M. Neurorestorative therapies for stroke: underlying mechanisms and translation to the clinic. Lancet Neurol. 2009;8(5):491–500.

64. Zheng W, Honmou O, Miyata K, Harada K, Suzuki J, Liu H, Houkin K, Hamada H, Kocsis JD. Therapeutic benefits of human mesenchymal stem cells derived from bone marrow after global cerebral ischemia. Brain Res. 2010;1310:8–16.

65. Zhu Y, Guan YM, Huang HL, Wang QS. Human umbilical cord blood mesenchymal stem cell transplantation suppresses inflammatory responses and neuronal apoptosis during early stage of focal cerebral ischemia in rabbits. Acta Pharmacol Sin. 2014;35(5):585–91.

66. Toma C, Wagner WR, Bowry S, Schwartz A, Villanueva F. Fate of culture-expanded mesenchymal stem cells in the microvasculature: in vivo observations of cell kinetics. Circ Res. 2009;104(3):398–402.

67. Xin H, Li Y, Chopp M. Exosomes/miRNAs as mediating cell-based therapy of stroke. Front Cell Neurosci. 2014;8:377.

68. Doeppner TR, Herz J, Görgens A, Schlechter J, Ludwig AK, Radtke S, de Miroschedji K, Horn PA, Giebel B, Hermann DM. Extracellular vesicles improve post-stroke neuroregeneration and prevent postischemic immunosuppression. Stem Cells Transl Med. 2015;4(10):1131–43.

69. Nalamolu KR, Venkatesh I, Mohandass A, Klopfenstein JD, Pinson DM, Wang DZ, Veeravalli KK. Exosomes treatment mitigates ischemic brain damage but does not improve post-stroke neurological outcome. Cell Physiol Biochem. 2019;52(6):1280–91.

70. Koh SH, Kim KS, Choi MR, Jung KH, Park KS, Chai YG, Roh W, Hwang SJ, Ko HJ, Huh YM, Kim HT, et al. Implantation of human umbilical cord-derived mesenchymal stem cells as a neuroprotective therapy for ischemic stroke in rats. Brain Res. 2008;1229:233–48.

71. Liao W, Xie J, Zhong J, Liu Y, Du L, Zhou B, Xu J, Liu P, Yang S, Wang J, Han Z, et al. Therapeutic effect of human umbilical cord multipotent mesenchymal stromal cells in a rat model of stroke. Transplantation. 2009;87(3):350–59.

72. Tanaka E, Ogawa Y, Mukai T, Sato Y, Hamazaki T, Nagamura-Inoue T, Harada-Shiba M, Shintaku H, Tsuji M. Dose-dependent effect of intravenous administration of human umbilical cord-derived mesenchymal stem cells in neonatal stroke mice. Front Neurol. 2018;9:133.

73. Clarkson ED, Zawada WM, Freed CR. GDNF reduces apoptosis in dopaminergic neurons in vitro. Neuroreport. 1995;7(1):145–49.

74. Esquenazi S, Monnerie H, Kaplan P, Le Roux P. BMP-7 and excess glutamate: opposing effects on dendrite growth from cerebral cortical neurons in vitro. Exp Neurol. 2002;176(1):41–54.

75. Harvey BK, Chang CF, Chiang YH, Bowers WJ, Morales M, Hoffer BJ, Wang Y, Federoff HJ. HSV amplicon delivery of glial cell line-derived neurotrophic factor is neuroprotective against ischemic injury. Exp Neurol. 2003;183(1):47–55.

76. Lein P, Johnson M, Guo X, Rueger D, Higgins D. Osteogenic protein-1 induces dendritic growth in rat sympathetic neurons. Neuron. 1995;15(3):597–605.

77. Zhang L, Ma Z, Smith GM, Wen X, Pressman Y, Wood PM, Xu XM. GDNF-enhanced axonal regeneration and myelination following spinal cord injury is mediated by primary effects on neurons. Glia. 2009;57(11):1178–91.

78. Abe K, Hayashi T. Expression of the glial cell line-derived neurotrophic factor gene in rat brain after transient MCA occlusion. Brain Res. 1997;776(1-2):230–34.

79. Chang CF, Lin SZ, Chiang YH, Morales M, Chou J, Lein P, Chen HL, Hoffer BJ, Wang Y. Intravenous administration of bone morphogenetic protein-7 after ischemia improves motor function in stroke rats. Stroke. 2003;34(2):558–64.

80. Harvey BK, Hoffer BJ, Wang Y. Stroke and TGF-beta proteins: glial cell line-derived neurotrophic factor and bone morphogenetic protein. Pharmacol Ther. 2005;105(2):113–25.

81. Acheson A, Conover JC, Fandl JP, DeChiara TM, Russell M, Thadani A, Squinto SP, Yancopoulos GD, Lindsay RM. A BDNF autocrine loop in adult sensory neurons prevents cell death. Nature. 1995;374(6521):450–53.

82. Ventimiglia R, Mather PE, Jones BE, Lindsay RM. The neurotrophins BDNF, NT-3 and NT-4/5 promote survival and morphological and biochemical differentiation of striatal neurons in vitro. Eur J Neurosci. 1995;7(2):213–22.

83. Waterhouse EG, An JJ, Orefice LL, Baydyuk M, Liao GY, Zheng K, Lu B, Xu B. BDNF promotes differentiation and maturation of adult-born neurons through GABAergic transmission. J Neurosci. 2012;32(41):14318–30.

84. Kowiański P, Lietzau G, Czuba E, Waśkow M, Steliga A, Moryś J. BDNF: a key factor with multipotent impact on brain signaling and synaptic plasticity. Cell Mol Neurobiol. 2018;38(3):579–93.

85. Mead B, Tomarev S. Bone marrow-derived mesenchymal stem cells-derived exosomes promote survival of retinal ganglion cells through miRNA-dependent mechanisms. Stem Cells Transl Med. 2017;6(4):1273–85.

86. Ahn SY, Sung DK, Kim YE, Sung S, Chang YS, Park WS. Brain-derived neurotropic factor mediates neuroprotection of mesenchymal stem cell-derived extracellular vesicles against severe intraventricular hemorrhage in newborn rats. Stem Cells Transl Med. 2021;10(3):374–84.

87. Zhang Y, Yi D, Hong Q, Cao J, Geng X, Liu J, Xu C, Cao M, Chen C, Xu S, Zhang Z, et al. Platelet-rich plasma-derived exosomes boost mesenchymal stem cells to promote peripheral nerve regeneration. J Control Release. 2024;367:265–82.

88. Song Y, Wang B. MiR-16 exacerbates neuronal cell growth and inhibits cell apoptosis by targeting AKT3 in cerebral ischemia injury. Trop J Pharm Res. 2021;20(10):2049–54.

89. Bernstein DL, Jiang X, Rom S. Let-7 microRNAs: their role in cerebral and cardiovascular diseases, inflammation, cancer, and their regulation. Biomedicines. 2021;9(6):606.

90. Pan J, Qu M, Li Y, Wang L, Zhang L, Wang Y, Tang Y, Tian HL, Zhang Z, Yang GY. MicroRNA-126-3p/-5p overexpression attenuates blood-brain barrier disruption in a mouse model of middle cerebral artery occlusion. Stroke. 2020;51(2):619–27.

91. Edbauer D, Neilson JR, Foster KA, Wang CF, Seeburg DP, Batterton MN, Tada T, Dolan BM, Sharp PA, Sheng M. Regulation of synaptic structure and function by FMRP-associated microRNAs miR-125b and miR-132. Neuron. 2010;65(3):373–84.

92. Wang P, Liang X, Lu Y, Zhao X, Liang J. MicroRNA-93 downregulation ameliorates cerebral ischemic injury through the Nrf2/HO-1 defense pathway. Neurochem Res. 2016;41(10):2627–35.

93. Son JW, Park J, Kim YE, Ha J, Park DW, Chang MS, Koh SH. Glia-like cells from late-passage human MSCs protect against ischemic stroke through IGFBP-4. Mol Neurobiol. 2019;56(11):7617–30.

94. Chou J, Harvey BK, Chang CF, Shen H, Morales M, Wang Y. Neuroregenerative effects of BMP7 after stroke in rats. J Neurol Sci. 2006;240(1–):21–29.

95. Kosaka N, Kodama M, Sasaki H, Yamamoto Y, Takeshita F, Takahama Y, Sakamoto H, Kato T, Terada M, Ochiya T. FGF-4 regulates neural progenitor cell proliferation and neuronal differentiation. Faseb J. 2006;20(9):1484–85.

96. Ahmed A, Nakagawa H, Isaksen TJ, Yamashita T. The effects of Bone Morphogenetic Protein 4 on adult neural stem cell proliferation, differentiation and survival in an in vitro model of ischemic stroke. Neurosci Res. 2022;183:17–29.

97. Magnoni S, Baker A, Thomson S, Jordan G, George SJ, McColl BW, McCulloch J, Horsburgh K. Neuroprotective effect of adenoviral-mediated gene transfer of TIMP-1 and -2 in ischemic brain injury. Gene Ther. 2007;14(7):621–25.

98. Tejima E, Guo S, Murata Y, Arai K, Lok J, van Leyen K, Rosell A, Wang X, Lo EH. Neuroprotective effects of overexpressing tissue inhibitor of metalloproteinase TIMP-1. J Neurotrauma. 2009;26(11):1935–41.

99. Frijns CJ, Kappelle LJ. Inflammatory cell adhesion molecules in ischemic cerebrovascular disease. Stroke. 2002;33(8):2115–22.

100. Tokami H, Ago T, Sugimori H, Kuroda J, Awano H, Suzuki K, Kiyohara Y, Kamouchi M, Kitazono T. RANTES has a potential to play a neuroprotective role in an autocrine/paracrine manner after ischemic stroke. Brain Res. 2013;1517:122–32.

101. England TJ, Gibson CL, Bath PM. Granulocyte-colony stimulating factor in experimental stroke and its effects on infarct size and functional outcome: a systematic review. Brain Res Rev. 2009;62(1):71–82.

102. Barone FC, Arvin B, White RF, Miller A, Webb CL, Willette RN, Lysko PG, Feuerstein GZ. Tumor necrosis factor-alpha. A mediator of focal ischemic brain injury. Stroke. 1997;28(6):1233–44.

103. Rose-John S, Jenkins BJ, Garbers C, Moll JM, Scheller J. Targeting IL-6 trans-signalling: past, present and future prospects. Nat Rev Immunol. 2023;23(10):666–81.

104. Barkholt L, Flory E, Jekerle V, Lucas-Samuel S, Ahnert P, Bisset L, Büscher D, Fibbe W, Foussat A, Kwa M, Lantz O, et al. Risk of tumorigenicity in mesenchymal stromal cell-based therapies—bridging scientific observations and regulatory viewpoints. Cytotherapy. 2013;15(7):753–59.

105. Janowski M, Lyczek A, Engels C, Xu J, Lukomska B, Bulte JW, Walczak P. Cell size and velocity of injection are major determinants of the safety of intracarotid stem cell transplantation. J Cereb Blood Flow Metab. 2013;33(6):921–27.

106. Ankrum JA, Ong JF, Karp JM. Mesenchymal stem cells: immune evasive, not immune privileged. Nat Biotechnol. 2014;32(3):252–60.

107. Kodali M, Castro OW, Kim DK, Thomas A, Shuai B, Attaluri S, Upadhya R, Gitai D, Madhu LN, Prockop DJ, Shetty AK. Intranasally administered human MSC-derived extracellular vesicles pervasively incorporate into neurons and microglia in both intact and status epilepticus injured forebrain. Int J Mol Sci. 2019;21(1):181.

108. Li J, Komatsu H, Poku EK, Olafsen T, Huang KX, Huang LA, Chea J, Bowles N, Chang B, Rawson J, Peng J, et al. Biodistribution of intra-arterial and intravenous delivery of human umbilical cord mesenchymal stem cell-derived extracellular vesicles in a rat model to guide delivery strategies for diabetes therapies. Pharmaceuticals (Basel). 2022;15(5):595.

109. Xian P, Hei Y, Wang R, Wang T, Yang J, Li J, Di Z, Liu Z, Baskys A, Liu W, Wu S, et al. Mesenchymal stem cell-derived exosomes as a nanotherapeutic agent for amelioration of inflammation-induced astrocyte alterations in mice. Theranostics. 2019;9(20):5956–75.

110. Zhang J, Buller BA, Zhang ZG, Zhang Y, Lu M, Rosene DL, Medalla M, Moore TL, Chopp M. Exosomes derived from bone marrow mesenchymal stromal cells promote remyelination and reduce neuroinflammation in the demyelinating central nervous system. Exp Neurol. 2022;347:113895.

111. Nozohouri S, Sifat AE, Vaidya B, Abbruscato TJ. Novel approaches for the delivery of therapeutics in ischemic stroke. Drug Discov Today. 2020;25(3):535–51.

112. Zhang S, Lachance BB, Moiz B, Jia X. Optimizing stem cell therapy after ischemic brain injury. J Stroke. 2020;22(3):286–305.

113. Tyson RJ, Park CC, Powell JR, Patterson JH, Weiner D, Watkins PB, Gonzalez D. Precision dosing priority criteria: drug, disease, and patient population variables. Front Pharmacol. 2020;11:420.

114. Sander O, Magnusson B, Ludwig I, Jullion A, Meille C, Lorand D, Bornkamp B, Hinder M, Kovacs SJ, Looby M. A framework to guide dose & regimen strategy for clinical drug development. CPT Pharmacometrics Syst Pharmacol. 2021;10(11):1276–80.

115. Fischer U, Koga M, Strbian D, Branca M, Abend S, Trelle S, Paciaroni M, Thomalla G, Michel P, Nedeltchev K, Bonati LH, et al. Early versus later anticoagulation for stroke with atrial fibrillation. N Engl J Med. 2023;388(26):2411–21.

116. Boehme AK, Esenwa C, Elkind MS. Stroke risk factors, genetics, and prevention. Circ Res. 2017;120(3):472–95.

117. Cipolla MJ, Liebeskind DS, Chan SL. The importance of comorbidities in ischemic stroke: impact of hypertension on the cerebral circulation. J Cereb Blood Flow Metab. 2018;38(12):2129–49.

118. Huang Y, Wang Z, Huang ZX, Liu Z. Biomarkers and the outcomes of ischemic stroke. Front Mol Neurosci. 2023;16:1171101.

119. El-Kadiry AE, Rafei M, Shammaa R. Cell therapy: types, regulation, and clinical benefits. Front Med (Lausanne). 2021;8:756029.

120. Nudo RJ, Wise BM, SiFuentes F, Milliken GW. Neural substrates for the effects of rehabilitative training on motor recovery after ischemic infarct. Science. 1996;272(5269):1791–94.

121. Witte OW, Bidmon HJ, Schiene K, Redecker C, Hagemann G. Functional differentiation of multiple perilesional zones after focal cerebral ischemia. J Cereb Blood Flow Metab. 2000;20(8):1149–65.

122. Cramer SC, Shah R, Juranek J, Crafton KR, Le V. Activity in the peri-infarct rim in relation to recovery from stroke. Stroke. 2006;37(1):111–15.